Supplementary Information (SI) for Journal of Materials Chemistry C.

Supporting Information

Converting aggregation-induced emission of N-BF_2 merocyanines to colour-tunable ultralong room temperature phosphorescence via Dexter triplet energy transfer: Circumventing restriction of intersystem crossing

Shan-Shan Gong,[a†] Xian-Zhi Tan,[a†] Rui-Xue Yang,[a] Chuan-Hui Cao,[a] Chunhong Zheng,[a] Yan-Xue Li,[a] He Zheng,[a] Gang Li,[a] Shouzhi Pu,*[b] Rongwei Shi,*[c] Zhao Chen,*[a] Qi Sun*[a]

[a]*Jiangxi Provincial Key Laboratory of Organic Functional Molecules, Institute of Organic Chemistry, Jiangxi Science and Technology Normal University, Nanchang, 330013, PR China.*
[b]*Department of Ecology and Environment, Yuzhang Normal University, Nanchang, 330103, PR China.*
[c]*School of Material and Chemical Engineering, Tongren University, Tongren, 554300, PR China.*
[†]*The authors contributed equally to this work.*

E-mails: pushouzhi@tsinghua.org.cn; njutshirongwei@163.com; 1020160936@jxstnu.edu.cn; sunqi@jxstnu.edu.cn

Table of contents

1. General methods Page S2–S3

2. Synthesis and characterization of **A1–A4** Page S4–S5

3. Photophysical data of **A1–A4** (Figs. S1–S3 and Table S1) Page S6

4. Theoretical and crystallographic investigations of **A1–A4** (and Figs. S4–S11 and Tables S2–S10) Page S7–S16

5. Photophysical data of **A1/BP–A4/BP** (Figs. S12–S17 and Table S11) Page S17–S19

6. Theoretical calculations of **A1/BP–A4/BP** (Figs. S18–S23 and Tables S11–S18) Page S19–S25

7. NMR and HRMS spectra of **A1–A4** (Figs. S24–S39) Page S26–S33

8. HPLC purity analysis of **A1–A4** (Figs. S40–S43) Page S34

1. General methods

1.1 Synthesis of **NBMCy-A1–A4**

All chemical reagents and solvents were obtained from commercial suppliers. All reactions were performed in commercial AR grade solvents without inert gas protection and monitored by thin layer chromatography on plates coated with 0.25 mm silica gel 60 F_{254}. TLC plates were visualized by UV irradiation (254 nm and 365 nm). Flash column chromatography employed silica gel (particle size 32–63 μm). NMR spectra were obtained with a Bruker AV-400 instrument with chemical shifts reported in parts per million (ppm, δ) and referenced to DMSO-d_6 and $CDCl_3$. ^{19}F NMR spectra were obtained with a Bruker AV-500 instrument. IR spectra were recorded on a Bruker Vertex-70 spectrometer. High-resolution mass spectra were obtained with a Bruker Dalton micrOTOF-Q II spectrometer and reported as *m*/*z*. Melting points were determined with a Tech X-4 melting point apparatus and uncorrected. HPLC traces of **A1**–**A4** were recorded on an Agilent 1260 Infinity LC system equipped with a YMC-Triart C18 analytical column (4.6 × 250 mm, 5 μm) [flow rate = 1.0 mL/min; 100% MeOH over 15 min; detection wavelengths at 400 nm (**A1**), 420 nm (**A2**, **A3**), and 500 nm (**A4**)].

1.2 UV-Vis, fluorescence, and phosphorescence spectrometry

Optical length of the quartz cell was 10 mm. Absorption spectra of solution samples of **A1**–**A4** (5×10^{-6} M) were recorded on an Agilent 8453 spectrophotometer. Absorption spectra of solid samples of **A1**–**A4** were recorded on a PerkinElmer Lambda 750 spectrophotometer. Fluorescence spectra of solution (5×10^{-5} M) and solid samples of **A1**–**A4** were recorded on a Hitachi F-4600 fluorescence spectrophotometer. Fluorescence lifetimes of **A1**–**A4** were recorded on a Hamamatsu compact fluorescence lifetime spectrometer C11367. Photoluminescent quantum yields of solution (5×10^{-5} M) and solid samples of **A1**–**A4** and **A1/BP**–**A4/BP** were determined on a Hamamatsu absolute PL quantum yield spectrometer C11347. Fluorescence and phosphorescence spectra, and phosphorescence lifetimes of **A1/BP**–**A4/BP** were recorded on an Edinburgh FLS1000 photoluminescence spectrometer.

1.3 Theoretical calculations

1.3.1 Geometry optimization

Ground- and excited-state geometry optimization and vertical excitation of **NBMCy-A1–A4** were carried out at B3LYP/6-311G (d, p) level of theory implemented on the Gaussian 16 package. Polarizable continuum model (PCM) was employed for solvent effect.

1.3.2 Molecular dynamics (MD) simulations

A 2.3×5.1×3.6 nm benzophenone (BP) unit cell with 180 BP molecules was built, and then an **A1–A4** molecule was placed in the position vacated by the two host molecules to obtain the initial models of **A1/BP–A4/BP**. For MD simulations, firstly, the energy minimizations were performed by using steepest descent algorithm and the conjugate gradient. Then, the 1 ns MD simulations under the NVT (T = 10 K) ensemble was performed. The temperature was controlled by the velocity rescaling thermostat. In the following step, the 10 ns MD simulations under the NPT (P = 1 bar, T = 10 K) ensemble coupled by Parrinello-Rahman barostat scheme was performed. The Newton's classical equations of motion were integrated at a time step of 2 fs using the classical leapfrog algorithm. All simulations and trajectory analysis were performed using the GROMACS (5.1.5) packages.

1.3.3 QM/MM calculations

The QM/MM calculations were carried out by the two-layered ONIOM method with the central molecule (in "VDW" model) as the high-layer QM part and the surrounding molecules (in "line" model) as the low-layer MM part. The initial model consists of 178 molecules for **BP**. One central molecule of **A1–A4** is defined as the QM region. The universal force field (UFF) was applied in the MM section, and the electrostatic embedding scheme was adopted in the QM/MM treatment. The optimized ground- and excited-state geometries in QM region were optimized with B3LYP/6-311G (d,p) basis set.

1.3.4 Spin-orbital coupling (SOC) calculations

The SOC constants of **A1**–**A4** in vacuum and doped systems between S_1 and triplet states were performed at B3LYP/6-311G (d,p) level of theory implemented on the ORCA (5.0.3) package.

1.3.5 Data analysis and visualization

The calculation data of hole-electron distribution, electronstatic potential (ESP) surface, Hirshfiled surface mapped with d_{norm} function and 2D fingerprint plots, Independent Gradient Model based on Hirshfeld Partition (IGMH), proportions of (n,π^*) and (π,π^*) configurations (α_n and β_π) at different states were analyzed by Multiwfn 3.8(dev). The results were visualized with Visual Molecular Dynamics (VMD) 1.9.3.

1.4 X-ray crystallographic analysis

Data collection for X-ray crystal analysis was performed on a Bruker Smart APEX-II single crystal X-ray diffractometer using graphite monochromated Mo-Kα radiation ($\lambda = 0.71073$ Å) at 296 K. The structures were solved by direct methods using SHELXL crystallographic software package. Crystallographic data of **A1**–**A4** are deposited in the Cambridge Crystallographic Data Centre (CCDC) and archived as Nos. 2241357, 224135, 2241364, and 2241365.

1.5 Photographs and videos

The daylight, fluorescence, and phosphorescence photographs and videos of **A1**–**A4** and **A1/BP**–**A4/BP** were taken by a HUAWEI Mate 60 Pro camera (50 MP, f/1.4-f/4.0). The quality of the videos was 1080p@30fps.

1.6 Doping methods for **A1/BP**–**A4/BP**

1.6.1 Solution-based method

This method is for the preliminary testing of the RTP properties of the doped systems. First, the guest was dissolved CH_2Cl_2 to prepare the guest stock solution at 10^{-3} M. The host was dissolved CH_2Cl_2 to prepare the host stock solution at 3×10^{-2} M. To acquire the doped samples at a certain molar ratio, the corresponding amounts of the host and guest stock solutions were mixed. The mixed solution was sonicated for 10 min at ambient temperature and slowly concentrated under reduced pressure and further dried under high vacuum. The samples should be subjected to microscopic analysis under both white light and 365 nm UV light to ensure homogeneity.

*When the doping molar ratio of **A1**–**A4** rises above 0.3%, the guest tends to aggregate, which in turn drastically lowers the concentration of **A1**–**A4** dispersed in the host.

1.6.2 Melt-casting method

This method may further enhance the RTP performance of the doped systems prepared by solution-based method. First, the doped sample prepared by solution-based method was heated to the melting point of the host in a RB flask. After the sample melt into a homogeneous solution, the hot liquid sample was transferred to a mould and slowly cooled to ambient temperature to solidify. **A1/BP**–**A4/BP** prepared by the melt-casting method typically show up as a crystalline solid.

2. Synthesis and characterization of **A1–A4**

2.1 General procedures for the synthesis of **A1–A4**

To a solution of 2,2-difluoro-1,3-dioxaboryl-pentadione (1.35 mmol) and 2-MeS-*N*-methylated or 4-Cl *N*-methylated benzoheterocyles (1.35 mmol) in dry DMF (2 mL) under argon was added TEA (2.03 mmol). The reaction was stirred for 30 min at 50 °C. Upon cooling, diisopropyl ether (20 mL) was added to the reaction. The precipitate was collected by filtration. Flash column chromatography on silica gel afforded **A1–A4** in pure form.

2.2 Characterization data of **A1–A4**

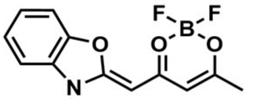

NBMCy-A1

2,2-Difluoro-6-methyl-4-((3-methylbenzo[d]oxazol-3-ium-2-yl)methylene)-4H-1,3,2-dioxaborinin-2-uide ***(NBMCy-A1)****.* The reaction of 2,2-difluoro-1,3-dioxaboryl-pentadione (200 mg, 1.35 mmol), 3-methyl-2-(methylthio)benzo[*d*]oxazol-3-ium trifluoromethanesulfonate (444 mg, 1.35 mmol) and TEA (284 µL, 2.03 mmol) followed by flash column chromatography (CH_2Cl_2/PE = 5:1) afforded **A1** (245 mg, 65%) as a light yellow solid; mp 208–209°C. ^{1}H NMR (400 MHz, DMSO-*d*$_6$): δ 7.77 (d, J = 7.8 Hz, 1H), 7.63 (d, J = 7.8 Hz, 1H), 7.46 (dd, J_1 = J_2 = 7.8 Hz, 1H), 7.40 (dd, J_1 = J_2 = 7.8 Hz, 1H), 5.64 (s, 1H), 5.32 (s, 1H), 3.66 (s, 3H), 2.00 (s, 3H) ppm; ^{13}C NMR (100 MHz, DMSO-*d*$_6$): δ 175.3, 174.1, 162.5, 146.8, 131.3, 126.3, 125.1, 111.5, 98.0, 74.2, 56.5, 30.8, 22.7 ppm; ^{19}F NMR (470 MHz, DMSO-*d*$_6$): δ -139.51 (s, 2F); IR (KBr): ν_{max} 3414, 2920, 2356, 2325, 1898, 1618, 1552, 1497, 1449, 1318, 1276, 1235, 1189, 1142, 1098, 1025, 968, 859, 833, 812, 757, 734 cm^{-1}; HRMS (ESI+): *m/z* calcd for $C_{13}H_{12}BF_2NO_3Na$ $[M+Na]^+$ 302.0771; found 302.0765.

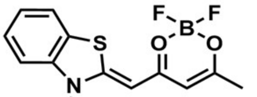

NBMCy-A2

2,2-Difluoro-6-methyl-4-((3-methylbenzo[d]thiazol-3-ium-2-yl)methylene)-4H-1,3,2-dioxaborinin-2-uide ***(NBMCy-A2)****.* The reaction of 2,2-difluoro-1,3-dioxaboryl-pentadione (200 mg, 1.35 mmol), 3-methyl-2-(methylthio)benzo[*d*]thiazol-3-ium perchlorate (398 mg, 1.35 mmol) and TEA (284 µL, 2.03 mmol) followed by flash column chromatography (CH_2Cl_2/PE = 3:1) afforded **A2** (223 mg, 56%) as a yellow solid. Mp 270–271°C. ^{1}H NMR (400 MHz, DMSO-*d*$_6$): δ 8.09 (d, J = 8.0 Hz, 1H), 7.78 (d, J = 8.0 Hz, 1H), 7.59 (dd, J_1 = J_2 = 8.0 Hz, 1H), 7.42 (dd, J_1 = J_2 = 8.0 Hz, 1H), 6.04 (s, 1H), 5.73 (s, 1H), 3.85 (s, 3H), 2.03 (s, 3H) ppm; ^{13}C NMR (100 MHz, DMSO-*d*$_6$): δ 173.3, 173.2, 163.6, 139.9, 127.5, 126.7, 124.5, 122.9, 113.1, 97.3, 86.5, 33.5, 22.2 ppm; ^{19}F NMR (470 MHz, DMSO-*d*$_6$): δ -139.73 (s, 2F); IR (KBr): ν_{max} 3436, 2921, 1608, 1595, 1558, 1464, 1439, 1413, 1250, 1176, 1058, 1026, 966, 803, 745 cm^{-1}; HRMS (ESI+): *m/z* calcd for $C_{13}H_{12}BF_2NO_2SNa$ $[M+Na]^+$ 318.0543; found 318.0537.

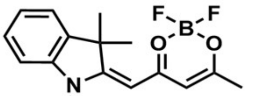

NBMCy-A3

*2,2-Difluoro-6-methyl-4-((1,3,3-trimethyl-3H-indol-1-ium-2-yl)methylene)-4H-1,3,2-dioxaborinin-2-uide (**NBMCy-A3**).* The reaction of 2,2-difluoro-1,3-dioxaboryl-pentadione (200 mg, 1.35 mmol), 1,3,3-trimethyl-2-(methylthio)-3*H*-indol-1-ium trifluoromethanesulfonate (480 mg, 1.35 mmol) and TEA (284 µL, 2.03 mmol) followed by flash column chromatography (CH_2Cl_2) afforded **A3** (152 mg, 37%) as a orange solid. Mp 185–186°C. ^{1}H NMR (400 MHz, $CDCl_3$): δ 7.38–7.27 (m, 2H), 7.24–7.13 (m, 1H), 7.03–6.89 (m, 1H), 5.60 (s, 1H), 5.06 (s, 1H), 3.39 (s, 3H), 2.11 (s, 3H), 1.76 (s, 6H) ppm; ^{13}C NMR (100 MHz, $CDCl_3$): δ 178.9, 177.8, 176.9, 142.1, 141.4, 128.0, 124.8, 122.4, 109.3, 99.8, 89.5, 50.4, 30.7, 24.1 (×2), 23.2 ppm; ^{19}F NMR (470 MHz, $CDCl_3$): δ -140.14 (s, 2F); IR (KBr): ν_{max} 3044, 2935, 1605, 1546, 1471, 1402, 1292, 1256, 1185, 1053, 1019, 825, 750 cm^{-1}; HRMS (ESI+): *m/z* calcd for $C_{16}H_{18}BF_2NO_2Na$ $[M+Na]^+$ 328.1291; found 328.1286.

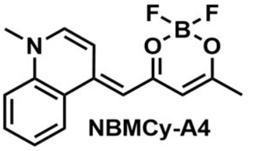

NBMCy-A4

*2,2-Difluoro-6-methyl-4-((1-methylquinolin-1-ium-4-yl)methylene)-4H-1,3,2-dioxaborinin-2-uide (**NBMCy-A4**).* The reaction of 2,2-difluoro-1,3-dioxaboryl-pentadione (200 mg, 1.35 mmol), 4-chloro-1-methylquinolin-1-ium perchlorate (373 mg, 1.35 mmol), and TEA (284 µL, 2.03 mmol) followed by flash column chromatography (CH_2Cl_2) afforded **A4** (140 mg, 36%) as a pink solid. Mp 251–252°C. ^{1}H NMR (400 MHz, DMSO-d_6): δ 8.47 (d, J = 8.6 Hz, 1H), 8.40 (d, J = 7.2 Hz, 1H), 8.23 (d, J = 7.2 Hz, 1H), 8.06–7.82 (m, 2H), 7.62 (dd, $J_1 = J_2$ = 7.0 Hz, 1H), 6.11 (s, 1H), 5.67 (s, 1H), 4.09 (s, 3H), 1.97 (s, 3H) ppm; ^{13}C NMR (100 MHz, DMSO-d_6): δ 173.0, 170.5, 151.3, 143.8, 138.2, 132.7, 126.3, 125.0, 123.5, 117.9, 111.1, 99.3, 91.7, 42.0, 22.1 ppm; ^{19}F NMR (470 MHz, DMSO-d_6): δ -139.81 (s, 2F); IR (KBr): ν_{max} 2924, 1528, 1485, 1456, 1411, 1373, 1345, 1295, 1274, 1257, 1236, 1190, 1127, 1054, 1020, 1001, 985, 923, 845, 810, 745, 519, 465 cm^{-1}; HRMS (ESI+): *m/z* calcd for $C_{15}H_{14}NO_2Na$ $[M+Na]^+$ 312.0978; found 312.0972.

3. Photophysical properties of **A1–A4**

3.1 Absorbance and emission spectra of **A1–A4**

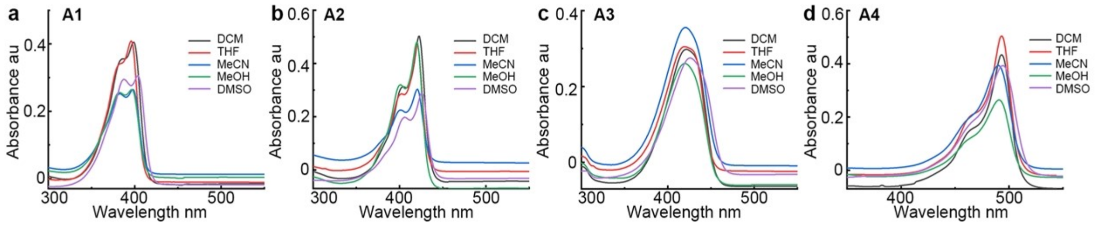

Fig. S1 UV-Vis absorbance spectra of **A1**–**A4** (a–d) in different organic solvents (5×10^{-6} M).

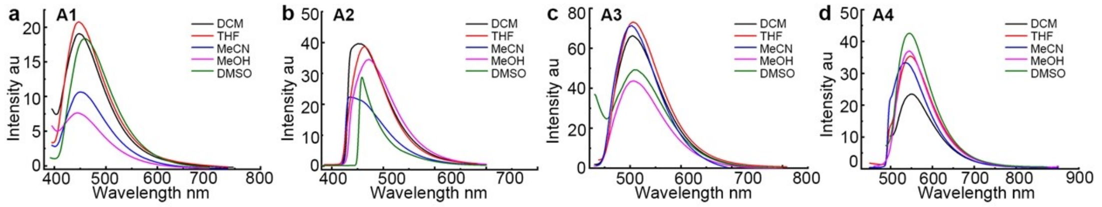

Fig. S2 PL spectra of **A1**–**A4** (a–d) in different organic solvents (5×10^{-5} M).

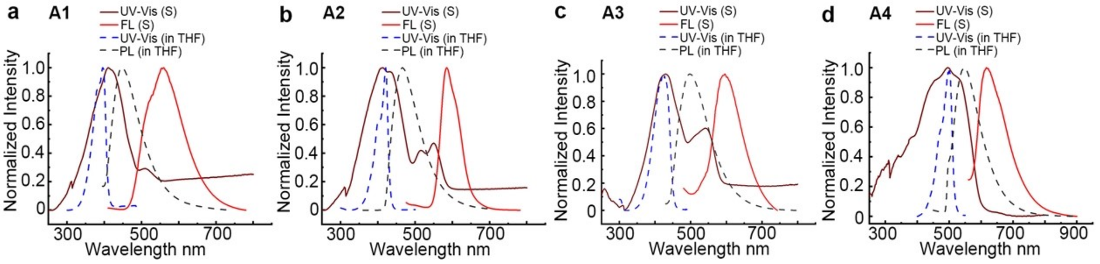

Fig. S3 UV-Vis absorbance and PL spectra of solution and solid samples of **A1**–**A4** (a–d).

3.2 Photophysical parameters of **A1**–**A4**

Table S1 Photophysical data of **A1**–**A4**[a]

Compd.	λ_{abs} (nm)		λ_{em} (nm)		Φ_F (%)		α_{AIE}	τ (ns) (k_r [10^8 s^{-1}], (k_{nr} [10^8 s^{-1}])
	soln (ε, 10^4)	solid[b]	soln ($\Delta\nu$)	solid ($\Delta\nu$)[b]	soln	solid[c]	$\Phi_{F,solid}/\Phi_{F,soln}$	solid[c]
A1	397 (8.1)	410	448 (2867)	556 (6405)	0.2	49.1	245.5	4.3 (1.14, 1.18)
A2	422 (10.1)	425	468 (2329)	584 (6406)	0.3	54.2	180.7	3.2 (1.69, 1.43)
A3	425 (5.6)	430	497 (3409)	596 (6477)	0.8	51.0	63.8	5.9 (0.86, 0.83)
A4	493 (8.6)	500	548 (2036)	612 (3660)	0.1	21.5	215.0	1.5 (1.43, 5.23)

[a] Abbreviations: soln = CH_2Cl_2 solution (5×10^{-6} M for UV-Vis and 5×10^{-5} M PL); ε = molar absorptivity ($M^{-1}cm^{-1}$); $\Delta\nu$ = Stokes shift (cm^{-1}); Φ_F = fluorescence quantum yield determined using a calibrated integrating sphere; α_{AIE} = value of AIE effect; τ = fluorescence lifetime measured at room temperature in air; k_r = radiative relaxation rate ($k_r = \Phi_F/\tau$); k_{nr} = non-radiative relaxation rate ($k_{nr} = (1-\Phi_F)/\tau$). [b] Determined on amorphous samples. [c] Determined on crystalline samples.

4. Theoretical and crystallographic investigations of **A1–A4**

4.1 Optimized geometries of **A1–A4** in ground state

Table S2 Molecular coordinates of **A1** in S_0 state

	X	Y	Z
N	-2.15876021	1.46785322	0.02183848
O	1.55055974	-0.59755144	-0.08059178
C	-0.96861822	0.80976964	0.00213595
C	-3.18917212	0.52449265	0.00228021
C	-2.56188300	-0.71689183	-0.03332254
C	1.52161771	0.71333115	-0.00175437
C	0.28863463	1.38892545	0.01989036
C	2.74638294	1.43819853	0.03102576
C	3.93950122	0.77452409	-0.08111960
O	4.00721356	-0.53910567	-0.16184074
F	2.79309154	-2.38691890	-0.92059625
C	-4.57499874	0.62145542	0.01087930
F	2.85926034	-1.93745086	1.32946211
C	-3.24547088	-1.91392951	-0.06276142
C	5.26379375	1.46396950	-0.14151648
C	-2.30875911	2.91889108	0.06096001
C	-5.28734981	-0.58036574	-0.01842810
C	-4.64120822	-1.82121198	-0.05445888
B	2.80636364	-1.38649665	0.04597437
H	-5.08571502	1.57478787	0.03915434
H	-6.36990896	-0.54707509	-0.01276994
H	-5.23070822	-2.72920839	-0.07616321
H	-2.72733713	-2.86315047	-0.09015308
H	0.32205091	2.46729290	0.05713923
H	2.72827970	2.51588099	0.09408413
H	5.15782086	2.54677941	-0.09620188
H	5.89218403	1.12646260	0.68779821
H	5.77657669	1.18946832	-1.06786016
H	-1.87238693	3.32014462	0.97688691
H	-1.82612090	3.37058514	-0.80673633
H	-3.36826782	3.15871520	0.03920934
O	-1.19314227	-0.52344228	-0.03379035

Table S3 Molecular coordinates of **A2** in S_0 state

	X	Y	Z
C	0.41940900	1.41189900	0.02525500
C	1.66820000	0.76900700	0.00248700
C	2.89062100	1.49310000	0.01105800
C	4.08178100	0.82445000	-0.10886500
C	5.40578100	1.51182100	-0.19963100
C	-0.80498600	0.75537700	0.00750700
O	1.69395000	-0.54473600	-0.05771400
O	4.14735800	-0.48806700	-0.17264900
B	2.95704300	-1.34224800	0.07555000
F	2.92584300	-2.35858900	-0.86593100
F	3.02292300	-1.84865200	1.37107300
S	-1.02002900	-0.98952900	-0.06323100
C	-2.77105100	-0.79524000	-0.04581400
C	-3.12845200	0.55833200	0.00733200
N	-2.00858700	1.39684300	0.04043700
C	-3.73413500	-1.79851600	-0.08112900
C	-5.07595300	-1.42907000	-0.06457100
C	-5.43771800	-0.07913800	-0.01495300
C	-4.47581600	0.92604900	0.02103100
C	-2.09123400	2.85634800	0.10606400
H	0.42578800	2.49098900	0.05393500
H	2.87330700	2.57167900	0.05805200
H	5.30202700	2.59549000	-0.16882900
H	6.04601800	1.18510100	0.62481000
H	5.90399300	1.22209200	-1.12918700
H	-3.44420700	-2.84119000	-0.12096600
H	-5.84248800	-2.19370700	-0.09143600
H	-6.48544800	0.19575800	-0.00464000
H	-4.78038500	1.96319600	0.05640000
H	-3.13127200	3.15437900	0.18446500
H	-1.55711700	3.22202200	0.98434500
H	-1.66290700	3.30108600	-0.79408200

Table S4 Molecular coordinates of **A3** in S_0 state

	X	Y	Z
C	0.38607000	1.31413800	0.00285100
C	1.67741900	0.73692400	-0.00898800
C	2.82734800	1.57009700	0.05569400
C	4.08366100	1.02114600	-0.01604700
C	5.33667800	1.83545400	-0.01807400
C	-0.86847700	0.72363400	-0.01840300
O	1.83878700	-0.55928400	-0.10099900
O	4.28075800	-0.27491800	-0.10116500
B	3.16158200	-1.24510800	0.00915100
F	3.25623800	-2.16511800	-1.02592100
F	3.22210800	-1.87292500	1.25215000
C	-1.29638400	-0.75664600	-0.02545700
C	-2.81052800	-0.63017800	-0.00420300
C	-3.16623400	0.71739500	0.00097300
N	-1.98972400	1.49688300	-0.01767800
C	-3.79406100	-1.60537300	0.00718000
C	-5.13800600	-1.21315400	0.02679100
C	-5.47751000	0.13898200	0.03488200
C	-4.49311700	1.13161100	0.02260900
C	-1.98473900	2.95390400	-0.02359200
C	-0.84548600	-1.48027300	-1.31706600
C	-0.80586100	-1.49891900	1.24022300
H	0.40683700	2.39436000	0.04380600
H	2.70998700	2.64085000	0.12579500
H	5.12650000	2.90250100	0.03711400
H	5.96325900	1.54464800	0.82993400
H	5.90676600	1.62481000	-0.92739700
H	-3.53357900	-2.65787100	0.00209500
H	-5.91817700	-1.96490000	0.03698700
H	-6.52072200	0.43198300	0.05207200
H	-4.77356500	2.17672600	0.03254100
H	-1.40960300	3.32699500	-0.87326700
H	-3.00450500	3.31637500	-0.11221900
H	-1.55249200	3.34298500	0.90153600
H	0.23695200	-1.57386600	-1.35339600
H	-1.28428900	-2.48076600	-1.33512500
H	-1.19072300	-0.94394300	-2.20399000
H	-1.22594300	-2.50755000	1.24707800
H	0.27878600	-1.57548000	1.25449400
H	-1.14144800	-0.98695700	2.14494600

Table S5 Molecular coordinates of **A4** in S_0 state

	X	Y	Z
O	-1.97027673	-0.70898748	0.06877515
C	2.23137085	0.69178375	-0.01224135
C	3.37744898	-0.15526531	0.01769242
N	3.21634290	-1.53380991	0.09000803
C	0.88543369	0.11620199	0.03391464
C	-2.63381941	1.55732384	0.02355475
H	-2.35834209	2.60093194	-0.01173424
O	-4.33364101	-0.06197350	0.20302104
C	-1.60887091	0.56159827	0.02387488
C	-3.94820533	1.20195258	0.15268724
C	4.67288122	0.39953048	-0.02631216
H	5.54071816	-0.24275070	-0.00296099
C	0.83367767	-1.30101251	0.10467338
H	-0.11690346	-1.80428798	0.14668111
C	-0.25674065	0.93595785	0.01314996
H	-0.11514934	2.00560668	-0.01363524
C	1.97107713	-2.05837854	0.12982545
H	1.91972944	-3.13689016	0.18643080
C	3.73160885	2.61680619	-0.13270127
H	3.86695394	3.68967696	-0.19222041
C	2.46040206	2.08424887	-0.08973778
H	1.61939955	2.76157303	-0.11851925
C	4.84519528	1.76605116	-0.09991987
H	5.84705051	2.17681269	-0.13312033
F	-3.61652913	-2.22507892	0.72572036
F	-3.55607765	-1.52292235	-1.45959171
C	-5.06467398	2.18827523	0.27319639
H	-5.60713027	2.01516741	1.20733348
H	-4.70062556	3.21455525	0.25499066
H	-5.77643037	2.04259506	-0.54476476
B	-3.37940347	-1.14676853	-0.12192515
C	4.37910080	-2.43150005	0.12585070
H	4.97559670	-2.31983847	-0.78041014
H	4.99753381	-2.21949655	0.99887860
H	4.01970145	-3.45488667	0.18804856

4.2 Vertical excitation of **A1–A4**

Table S6 Selected parameters for the vertical excitation of **A1**

Electronic transition	Energy, eV/λ nm	f[a]	Composition[b]	CI[c]	Contribution
$S_0 \rightarrow S_1$	3.45/359	1.2142	H→L	0.70567	99%
$S_0 \rightarrow S_2$	4.23/293	0.0181	H–2→L	0.15198	5%
			H–1→L	0.54745	60%
			H→L+1	-0.40837	33%
$S_0 \rightarrow S_3$	4.66/266	0.0049	H–2→L	0.50225	50%
			H–1→L	-0.33460	22%
			H→L+2	-0.27302	15%
$S_0 \rightarrow S_4$	4.76/261	0.0217	H–2→L	0.35779	26%
			H–1→L	0.26909	14%
			H→L+1	0.50338	51%

Table S7 Selected parameters for the vertical excitation of **A2**

Electronic transition	Energy, eV/λ nm	f[a]	Composition[b]	CI[c]	Contribution
$S_0 \rightarrow S_1$	3.33/373	1.1268	H→L	0.70599	99%
$S_0 \rightarrow S_2$	4.23/293	0.0181	H–1→L	0.62083	77%
			H→L+1	0.30291	18%
$S_0 \rightarrow S_3$	4.52/275	0.0562	H–2→L	0.18703	7%
			H–1→L	-0.26257	14%
			H→L+1	0.60152	72%
$S_0 \rightarrow S_4$	4.59/270	0.0185	H–2→L	0.65189	85%
			H–2→L	0.16467	5%
			H→L+1	-0.12927	3%

Table S8 Selected parameters for the vertical excitation of **A3**

Electronic transition	Energy, eV/λ nm	f[a]	Composition[b]	CI[c]	Contribution
$S_0 \rightarrow S_1$	3.21/386	0.9383	H→L	0.70486	99%
$S_0 \rightarrow S_2$	4.25/292	0.0781	H–2→L	-0.41981	35%
			H–1→L	0.51621	53%
			H→L+1	-0.21700	9%
$S_0 \rightarrow S_3$	4.36/284	0.1111	H–2→L	0.45161	41%
			H–1→L	0.46697	44%
			H→L+2	0.24669	12%
$S_0 \rightarrow S_4$	4.64/267	0.1022	H–2→L	-0.33238	22%
			H–2→L+2	-0.11219	3%
			H→L+1	0.60731	74%

Table S9 Selected parameters for the vertical excitation of **A4**

Electronic transition	Energy, eV/λ nm	f^a	Composition^b	CI^c	Contribution
$S_0 \rightarrow S_1$	3.80/443	0.8592	H→L	0.70611	99%
			H–2→L	0.19201	7%
$S_0 \rightarrow S_2$	3.80/327	0.0027	H–1→L	0.45913	42%
			H→L+1	0.49301	49%
			H–2→L	-0.13279	4%
$S_0 \rightarrow S_3$	3.90/318	0.0158	H–1→L	-0.47343	45%
			H→L+1	0.48773	48%
			H–2→L	0.64838	84%
$S_0 \rightarrow S_4$	4.13/300	0.0015	H–1→L	-0.21938	10%
			H→L+2	-0.14222	4%

^{a}Oscillator strength. ^{b}H, HOMO (highest occupied molecular orbital) and L, LUMO (lowest unoccupied molecular orbital). ^{c}Coefficient of wavefunction.

4.3 Theoretical and crystallographic analysis of **A1**, **A2** and **A4**

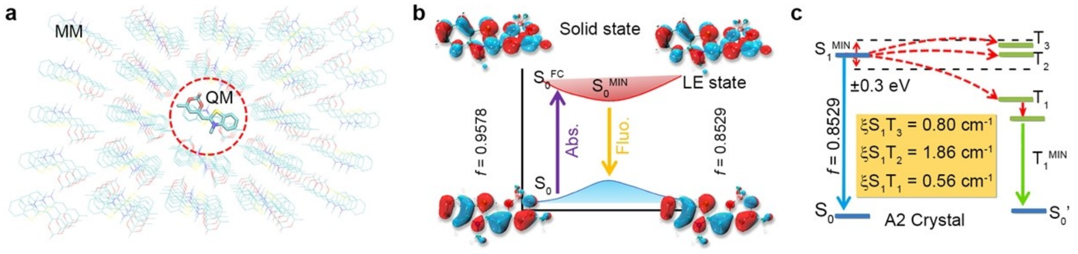

Fig. S4 (a) Setup of the QM/MM model for a cluster with 119 **A2**. (b) The excitation and decay characteristics of **A2** in solid state. (c) SOC and energy level calculations of **A2** in single crystal.

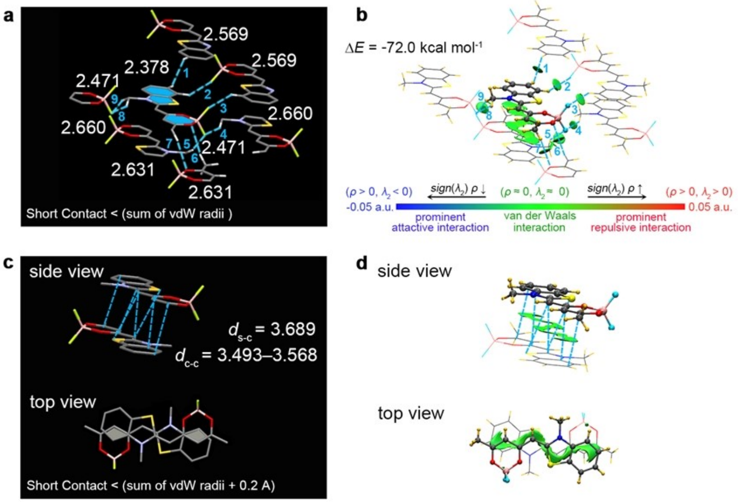

Fig. S5 (a,c) Short contacts determined by Mercury software peripheral to the center molecule and between two slip-stacked **A2** molecules at different short contact definitions. (b,d) The visualization of molecular interactions by IMGH method corresponding to the two groups of short contacts in Figs S5a and S5c. Insets: Calculated mean interaction energy (*ΔE*) of **A2** in single crystal and annotation of common interpretation of sign(λ_2)ρ in different value ranges and the coloring method.

* The calculation result of the single crystal of **A2** well agrees with the interactions identified by the crystallographic analysis software (Mercury 4.2.0). The green isosurfaces indicate that all these interactions are van der Warrs (vdW) interactions. Interestingly, the IGMH calculation showed that vdW interactions exist between the edges of the two slip-stacked **A2** molecules. However, when the short contact was defined as the interatomic distance < sum of vdW radii, these interactions were not shown as other short contacts by the Mercury software. Only after the short contact definition was changed to interatomic distance < (sum of vdW radii + 0.2 Å) was these interactions indicated by the Mercury software. Moreover, in agreement with the crystallographic analysis, no π-π overlap was indicated by the theoretical calculations.

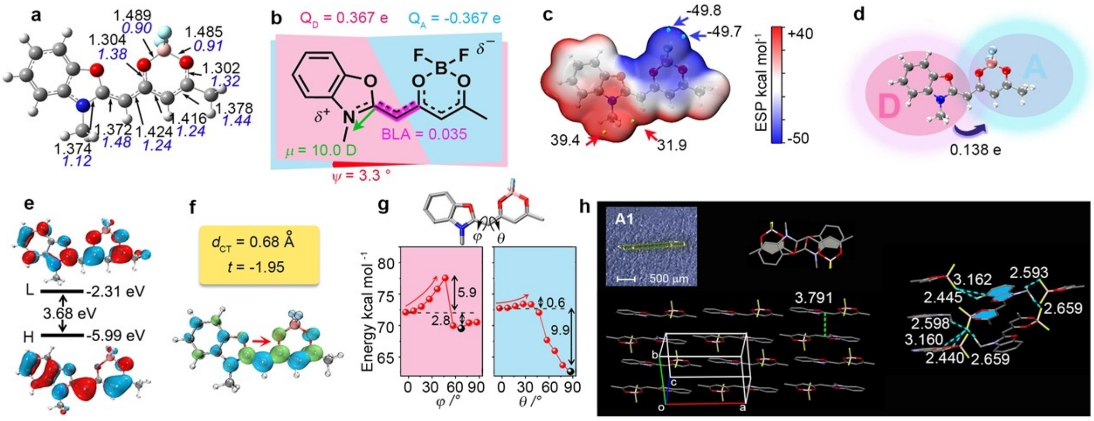

Fig. S6 (a) Bond lengths (black) and orders (blue) of **A1** in optimized ground-state geometry. (b) Partial charges and dihedral angel of two fragments, BLA value of monomethine, and dipole moment of **A1**. (c) ESP surface of **A1**. (d) IFCT of **A1**. (e) Molecular orbital amplitude plots of HOMO and LUMO energy levels of **A1**. (f) Hole-electron distribution of **A1** (blue: holes; green: electrons; isosurface: 0.003) with d_{CT} (red arrow) and *t* indices. (g) PECs of S_1 state of **A1** as a function of *φ* and *θ* (The dark state is label as black spot). (h) Crystallographic analysis of **A1** (*d*, Å).

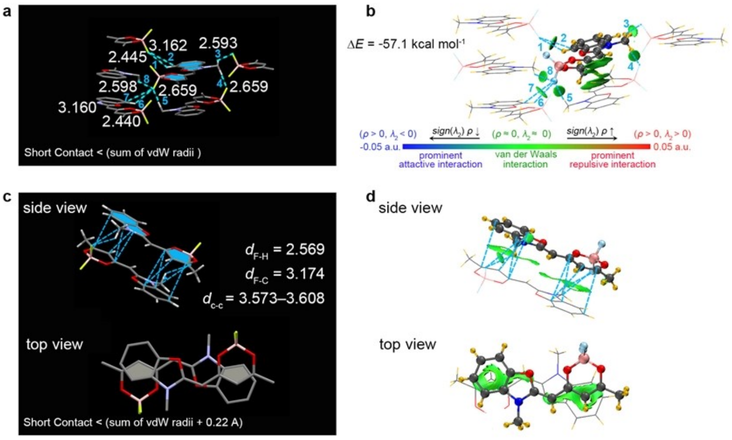

Fig. S7 (a,c) Short contacts determined by Mercury software peripheral to the center molecule and between two slip-stacked **A1** molecules at different short contact definitions. (b,d) The visualization of molecular interactions by IMGH method corresponding to the two groups of short contacts in Figs S7a and S7c. Insets: the calculated mean interaction energy (*ΔE*) of **A1** in single crystal and annotation of common interpretation of sign(λ_2)ρ in different value ranges and the coloring method.

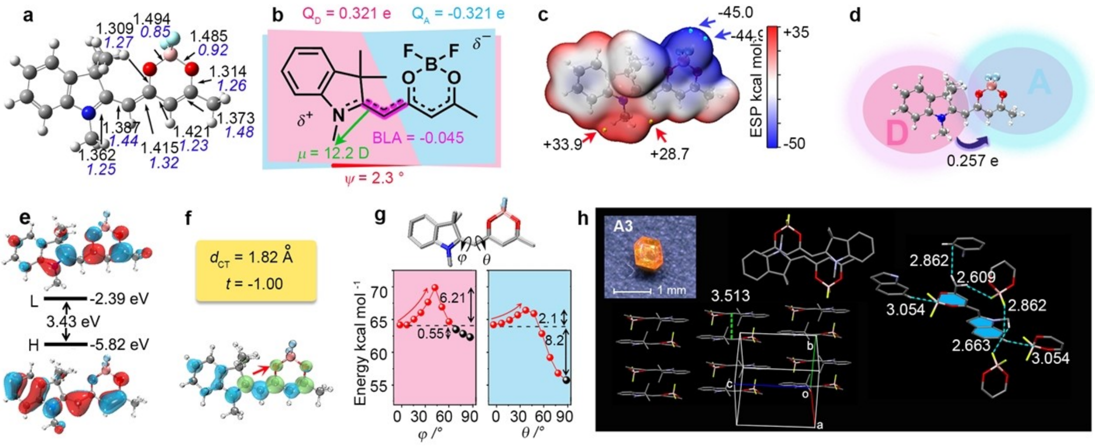

Fig. S8 (a) Bond lengths (black) and orders (blue) of **A3** in ground-state geometry. (b) Partial charges and dihedral angel of two fragments, BLA value of monomethine, and dipole moment of **A3**. (c) ESP surface of **A3**. (d) IFCT of **A3**. (e) Molecular orbital amplitude plots of HOMO and LUMO energy levels of **A3**. (f) Hole-electron distribution of **A3** (blue: holes; green: electrons; isosurface: 0.003) with d_{CT} (red arrow) and t indices. (g) PECs of S_1 state of **A3** as a function of φ and θ (The dark state is label as black spot). (h) Crystallographic analysis of **A3** (d, Å).

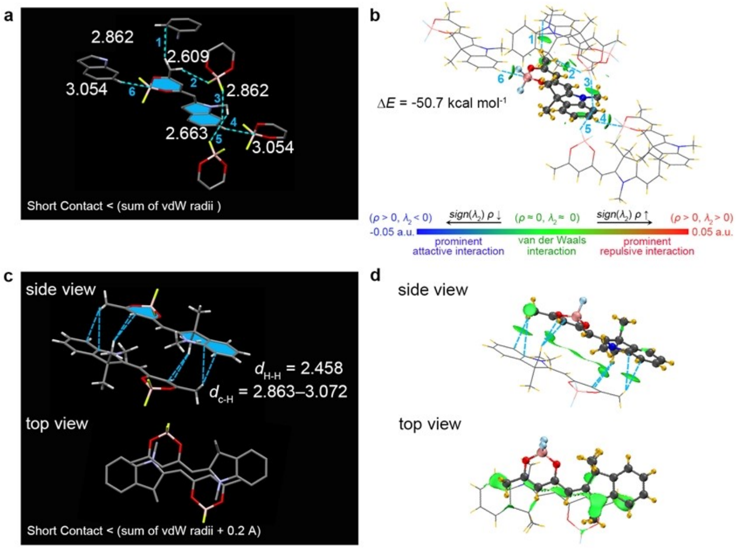

Fig. S9 (a,c) Short contacts determined by Mercury software peripheral to the center molecule and between two slip-stacked **A3** molecules at different short contact definitions. (b,d) The visualization of molecular interactions by IMGH method corresponding to the two groups of short contacts in Figs S9a and S9c. Insets: the calculated mean interaction energy (ΔE) of **A3** in single crystal and annotation of common interpretation of sign(λ_2)ρ in different value ranges and the coloring method.

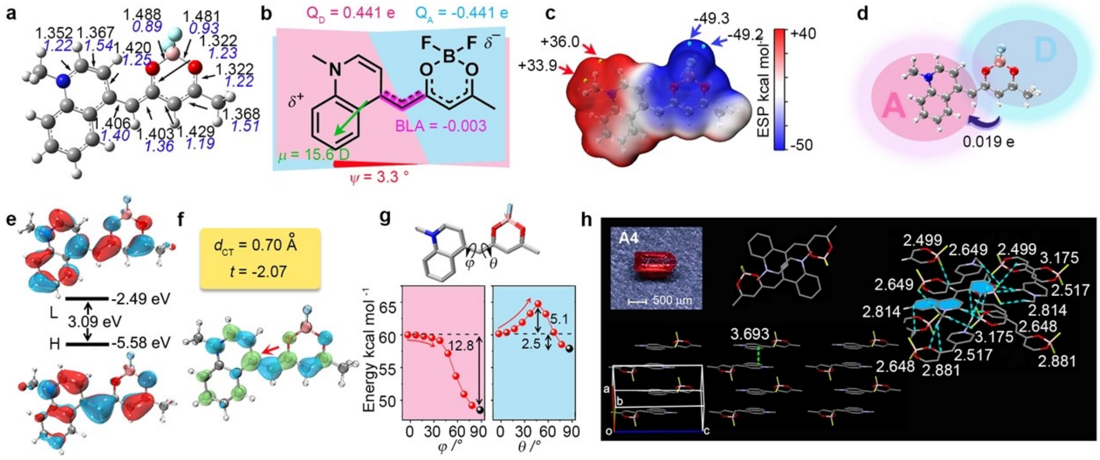

Fig. S10 (a) Bond lengths (black) and orders (blue) of **A4** in ground-state geometry. (b) Partial charges and dihedral angel of two fragments, BLA value of monomethine, and dipole moment of **A4**. (c) ESP surface of **A4**. (d) IFCT of **A4**. (e) Molecular orbital amplitude plots of HOMO and LUMO energy levels of **A4**. (f) Hole-electron distribution of **A4** (blue: holes; green: electrons; isosurface: 0.003) with d_{CT} (red arrow) and *t* indices. (g) PECs of S_1 state of **A4** as a function of *φ* and *θ* (The dark state is labelled in black). (h) Crystallographic analysis of **A4** (*d*, Å).

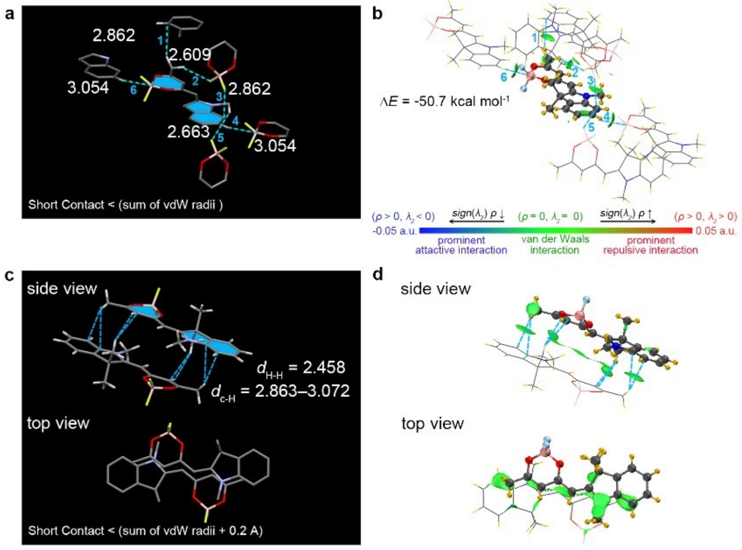

Fig. S11 (a,c) Short contacts determined by Mercury software peripheral to the center molecule and between two slip-stacked **A4** molecules at different short contact definitions. (b,d) The visualization of molecular interactions by IMGH method corresponding to the two groups of short contacts in Figs S11a and S11c. Insets: the calculated mean interaction energy (*ΔE*) of **A4** in single crystal and annotation of common interpretation of sign(λ_2)*ρ* in different value ranges and the coloring method.

4.4 Single crystal data of **A1–A4**

Table S10 Single crystal data of **A1**–**A4**

	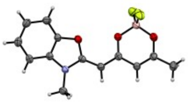 **A1**	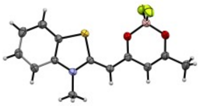 **A2**	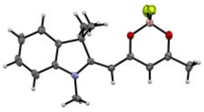 **A3**	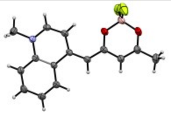 **A4**
CCDC Number	**2241357**	**2241364**	**2241365**	**2241358**
Formula	$C_{13}H_{12}BF_2NO_3$	$C_{13}H_{12}BF_2NO_2S$	$C_{16}H_{18}BF_2NO_2$	$C_{15}H_{14}BF_2NO_2$
Formula weight	279.05	295.11	305.12	289.26
Temperature (K)	296(2)	296(2)	296(2)	296(2)
Crystal system	monoclinic	triclinic	triclinic	monoclinic
Space group	P 1 21/c 1	P-1	P-1	P 1 21/c 1
Unit cell dimensions				
a (Á)	11.999(2)	6.9969(11)	10.8745(16)	7.2283(7)
b (Á)	7.0595(12)	7.6998(12)	11.4234(16)	12.3581(13)
c (Á)	15.590(3)	12.488(2)	12.5897(17)	15.0616(17)
α (°)	90	78.223(3)	88.109(2)	90
β (°)	102.040(3)	83.171(3)	85.998(2)	92.076(2)
γ (°)	90	84.636(3)	89.550(3)	90
Volume (Á^3)	1291.5(4)	652.27(18)	1559.3(4)	1344.5(2)
Z	4	1	4	4
Density(calcd)(g/cm^3)	1.435	1.503	1.300	1.428
Goodness-of-fit on F^2	1.024	1.037	1.018	1.0523
Final R indices [I/2σ(I)]				
R1	0.0457	0.0457	0.0516	0.0536
w R2	0.1066	0.1158	0.1166	0.1092
R indices (all data)				
R1	0.0798	0.0601	0.1026	0.1121
w R2	0.1227	0.1255	0.1424	0.1351

5. Photophysical properties of **A1/BP–A4/BP**

5.1 Optimization of doping molar ratio

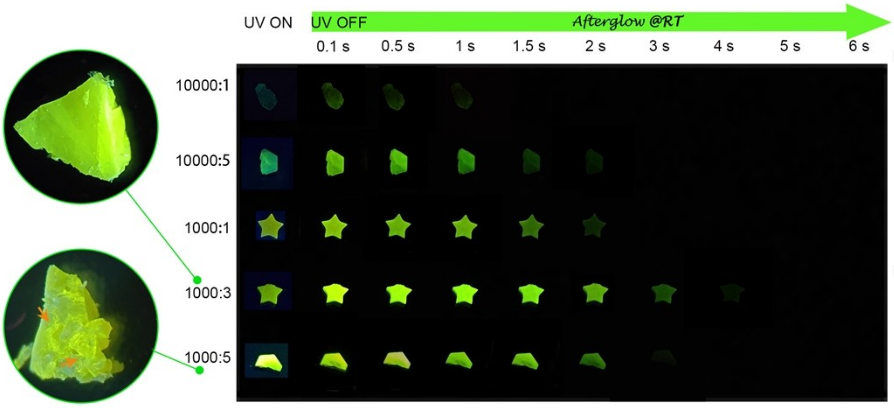

Fig. S12 The photographs of the afterglows of **A2/BP** samples with various doping molar ratios. Insets: The microscopic images of the samples with 1000:3 and 1000:5 molar ratios. (**A2** aggregations are pointed out with orange arrows.)

5.2 Absorbance and PL properties of **A1/BP**, **A2/BP**, and **A4/BP**

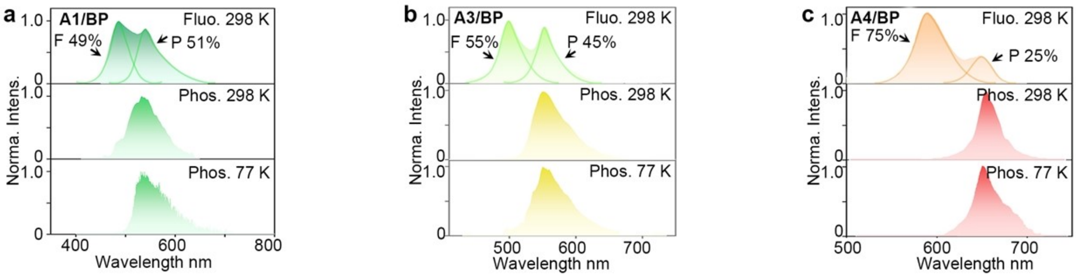

Fig. S13 The steady-state and prompt emission spectra of **A1/BP** (a), **A3/BP** (b), and **A4/BP** (c) at 298 K and 77 K.

Table S11 Photophysical data of **A1/BP–A4/BP**

H-G system	λ_{em} (nm)		Φ (%)			τ_p (ms)
	Fluo.	Phos.	Φ_{PL}	Φ_F	Φ_P	
A1/BP	483	531	5.8	2.8	3.0	115.3
A2/BP	480	542	18.3	2.4	15.9	360.3
A3/BP	498	553	8.9	4.8	4.1	523.8
A4/BP	565	652	3.2	2.4	0.8	159.3

[a] Abbreviations: Φ_{PL} = photoluminescence quantum yield determined using a calibrated integrating sphere; Φ_F = fluorescence quantum yield; Φ_P = phosphorescence quantum yield; τ_P = phosphorescence lifetime measured at room temperature in air.

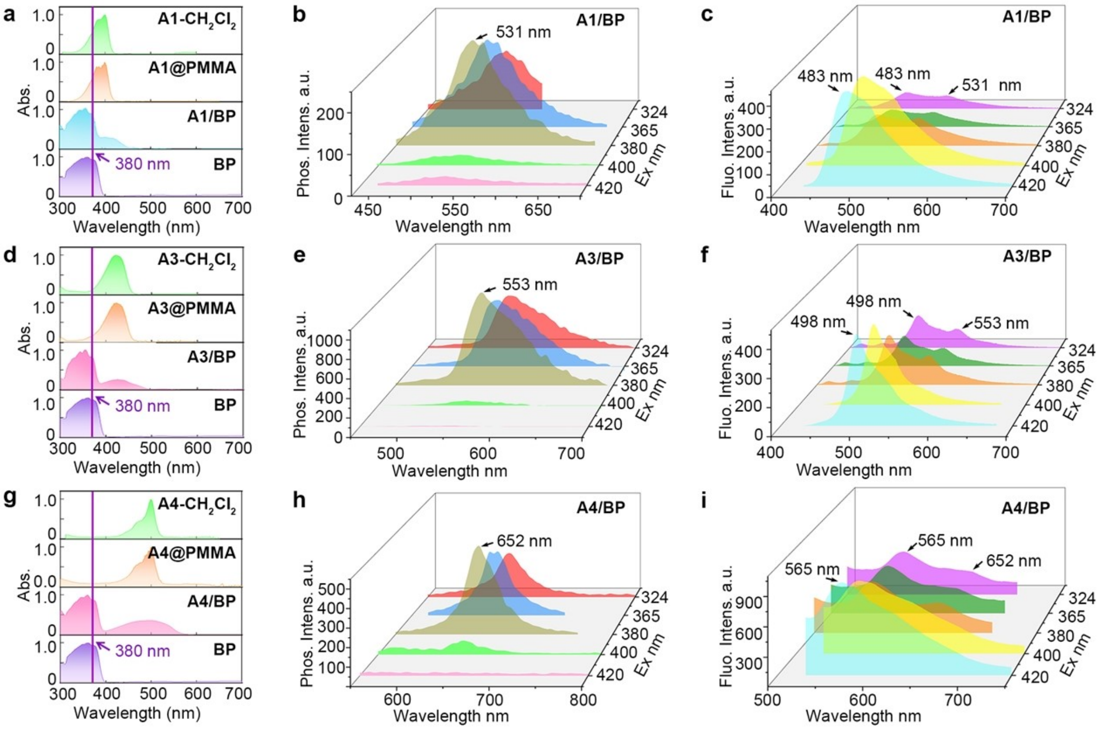

Fig. S14 Stacked absorption spectra of **A1** (a), **A3** (d), and **A4** (g) in isolated states and BP in aggregated state. Stacked prompt emission spectra of **A1/BP** (b), **A3/BP** (e), and **A4/BP** (h) with different excitation wavelengths. Stacked steady-state emission spectra of **A1/BP** (c), **A3/BP** (f), and **A4/BP** (i) with different excitation wavelengths.

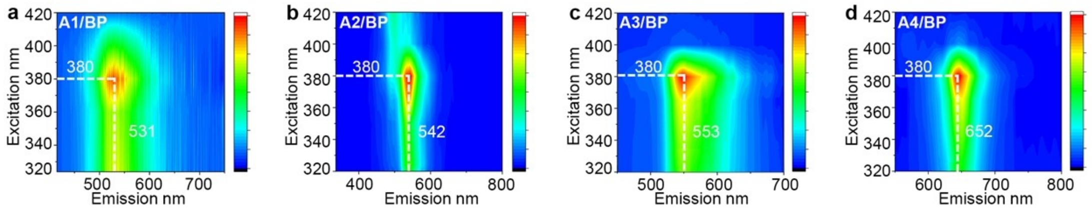

Fig. S15 2D Excitation-phosphorescence maps of **A1/BP–A4/BP** (a–d).

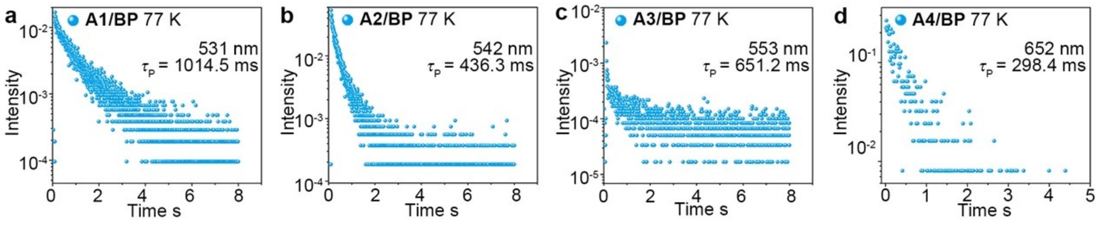

Fig. S16 Phosphorescence decay diagrams of **A1/BP–A4/BP** (a–d) at 77 K.

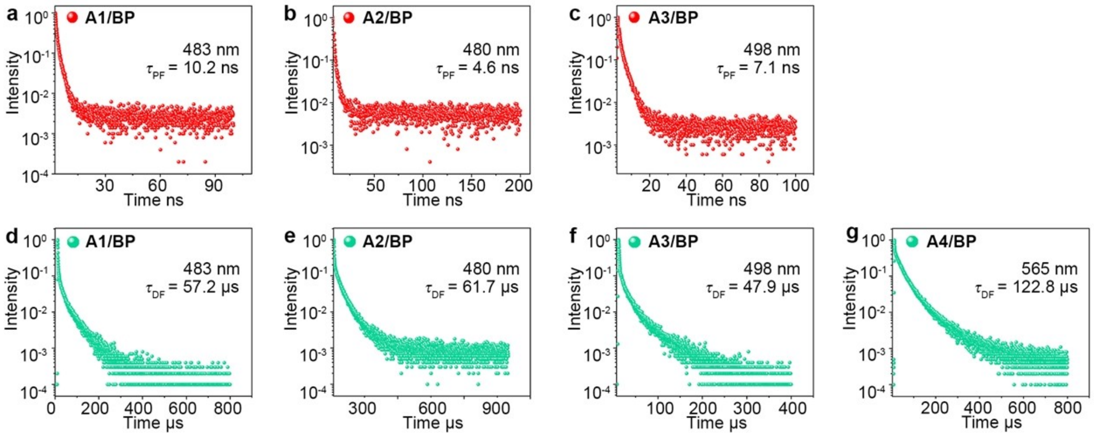

Fig. S17 Fluorescence decay diagrams of **A1/BP–A3/BP** (a–c) at ns range and **A1/BP–A4/BP** (d–g) at μs range.

6. Theoretical calculations of **A1/BP–A4/BP**

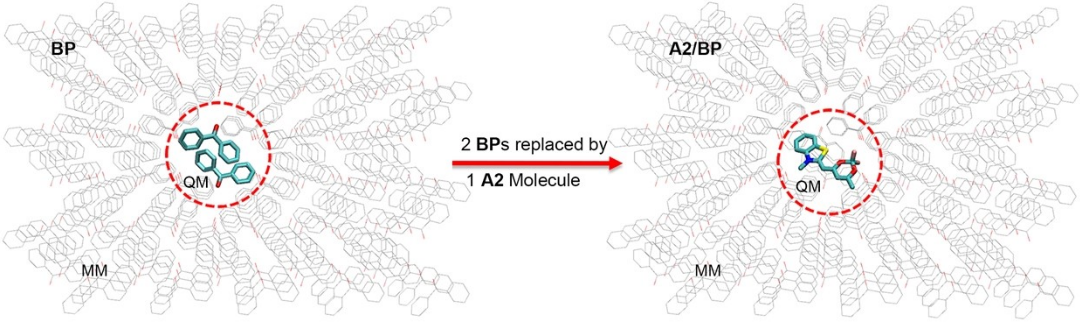

Fig. S18 Model setup for molecular dynamics (MD) simulations and QM/MM calculations of **A2/BP**.

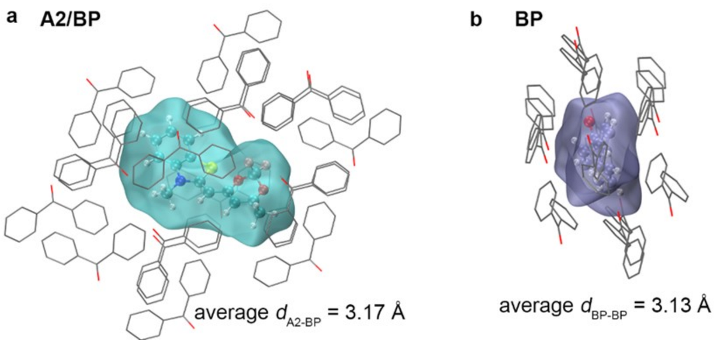

Fig. S19 Calculated the average molecular distances between the central molecules and surrounding BP molecules in **A2/BP** (a) and BP single crystal (b).

Table S12 Molecular coordinates of **A2** in MD simulated **A2/BP** model

	X	Y	Z
S	6.62400000	33.82200000	18.20000000
O	8.66000000	35.24000000	16.64800000
N	7.68500000	31.37400000	18.30500000
F	10.38800000	36.46300000	17.60800000
O	10.01800000	36.63400000	15.34200000
F	8.52300000	37.52300000	16.84700000
C	7.85700000	32.62300000	17.68000000
C	8.83900000	32.92500000	16.76400000
C	6.92100000	31.53100000	19.44900000
C	10.59400000	35.65900000	14.94600000
C	6.85200000	30.61200000	20.50500000
C	9.20800000	34.23000000	16.26100000
C	10.17500000	34.34600000	15.35500000
C	6.28300000	32.76200000	19.55500000
C	6.12600000	30.94300000	21.66000000
C	5.49100000	32.20600000	21.75900000
C	5.54600000	33.11900000	20.68100000
C	8.36000000	30.11200000	17.92900000
C	11.75400000	35.73000000	14.03500000
B	9.41200000	36.52100000	16.68400000
H	5.06700000	34.09100000	20.75200000
H	4.95800000	32.45600000	22.67200000
H	6.09400000	30.24900000	22.49500000
H	7.35800000	29.65200000	20.46700000
H	9.49000000	32.10100000	16.48200000
H	10.68400000	33.47100000	14.95600000
H	9.31200000	30.03700000	18.46800000
H	8.50100000	30.07000000	16.84100000
H	7.73400000	29.25500000	18.20700000
H	11.70800000	36.67500000	13.48100000
H	11.73400000	34.89000000	13.33000000
H	12.67300000	35.69200000	14.63300000

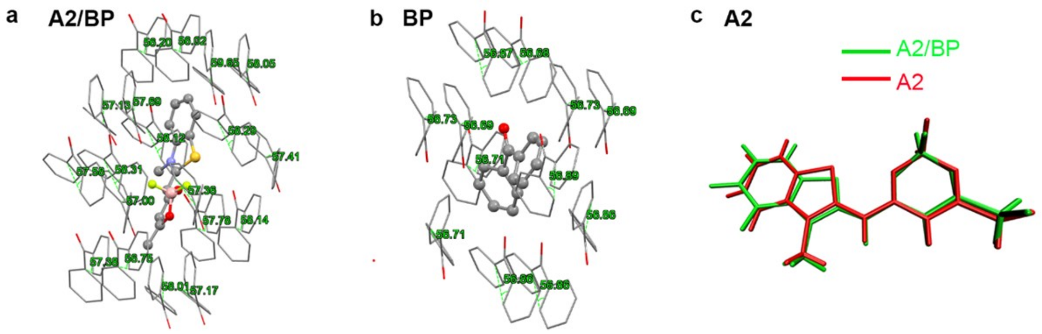

Fig. S20 The molecular conformations of surrounding BPs in **A2/BP** (a) and those of surrounding BPs in BP single crystals (b). The superimposition of **A2**’s geometries in **A2/BP** and **A2** single crystals by aligning the coordinates of all atoms (c).

Table S13 Molecular coordinates of **A2** in S$_1$ state of **A2/BP** model (QM/MM method)

	X	Y	Z
S	8.60753700	0.74218400	-5.24945800
O	9.91641500	-0.69961200	-3.39292300
N	6.09981200	0.58898300	-4.45841600
F	11.06554600	0.29680100	-1.61471300
O	11.47262100	-1.95997000	-1.98153700
F	12.21055500	-0.32219700	-3.51213300
C	7.35281200	-0.00645000	-4.21596900
C	7.58754200	-0.98319900	-3.28889400
C	6.13598300	1.66286300	-5.30561900
C	10.45963500	-2.64490400	-1.50823900
C	5.08424300	2.53832200	-5.62264100
C	8.91414600	-1.39151700	-2.87453500
C	9.15123200	-2.39780900	-1.93895000
C	7.42804600	1.87423300	-5.86705600
C	5.34323900	3.59772100	-6.47676700
C	6.61992500	3.80681000	-7.02506300
C	7.66653400	2.94236600	-6.72904900
C	4.94548700	0.24467700	-3.64745400
C	10.79329500	-3.61287900	-0.43484500
B	11.21476900	-0.62651500	-2.63051600
H	8.65582100	3.10430400	-7.14001100
H	6.79135100	4.65720800	-7.66887300
H	4.54030500	4.28278400	-6.71246000
H	4.09749500	2.41318300	-5.19812400
H	6.75209500	-1.43330600	-2.76846200
H	8.33261800	-2.97449000	-1.53339300
H	5.04103900	0.64495800	-2.63158100
H	4.84038100	-0.83910900	-3.59186300
H	4.05035300	0.64819100	-4.11227800
H	11.74339800	-4.10330400	-0.65271500
H	10.00957600	-4.35461500	-0.28886100
H	10.92734300	-3.06810100	0.50737500

Table S14 Molecular coordinates of **A2** in T_1 state of **A2/BP** model (QM/MM method)

	X	Y	Z
S	8.62424300	0.80390500	-5.20303100
O	9.92464200	-0.72124900	-3.40791400
N	6.15893300	0.60717600	-4.42945900
F	11.12446400	0.31293300	-1.68163100
O	11.46392200	-1.96394100	-1.96715100
F	12.22727800	-0.40669400	-3.56649700
C	7.38782800	0.04553300	-4.20016000
C	7.61390100	-0.97550300	-3.29723400
C	6.16079700	1.69217500	-5.31007800
C	10.43108300	-2.59595900	-1.48600600
C	5.09097400	2.52679100	-5.63289300
C	8.90866000	-1.34309400	-2.86969700
C	9.13903000	-2.32159700	-1.87630700
C	7.43130000	1.92735800	-5.85212300
C	5.32344600	3.59653400	-6.49030700
C	6.59150500	3.83322500	-7.02335000
C	7.65788200	2.99546100	-6.71218200
C	4.99479200	0.23065800	-3.63952100
C	10.75556300	-3.60204000	-0.43667000
B	11.24364600	-0.64865400	-2.65906700
H	8.64601100	3.17941900	-7.11697100
H	6.75244800	4.68332500	-7.67043700
H	4.50214700	4.25742100	-6.73149200
H	4.10404300	2.37547400	-5.21592000
H	6.77543200	-1.44339200	-2.80318100
H	8.31376500	-2.87263100	-1.45359800
H	5.07704400	0.60954900	-2.61621200
H	4.89527200	-0.85406100	-3.61108800
H	4.10395900	0.64038600	-4.10611200
H	11.70242700	-4.08645700	-0.67055900
H	9.96553400	-4.33930300	-0.31086700
H	10.88538700	-3.07123300	0.50967800

Table S15 Calculated configuration proportions of α_n and β_π of **A1**'s various states based on MPA

S_1^{MIN}						T_1^{MIN}					
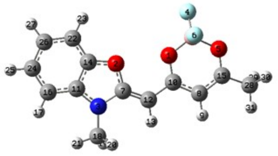						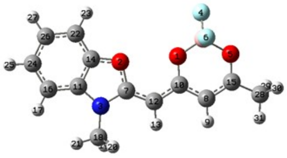					
HOMO			LOMO			HOMO			LOMO		
Type	Atom	Total	Type	Atom	Total	Type	Atom	Total	Type	Atom	Total
Z	2(O)	1.47%	Z	1(O)	2.15%	Z	2(O)	1.27%	Z	1(O)	1.81%
Z	2(O)	2.56%	Z	1(O)	3.58%	Z	2(O)	2.19%	Z	1(O)	3.01%
Z	2(O)	1.13%	Z	1(O)	1.94%	Z	2(O)	0.93%	Z	1(O)	1.63%
Z	3(N)	3.37%	Z	2(O)	0.87%	Z	3(N)	2.62%	Z	2(O)	1.09%
Z	3(N)	6.25%	Z	2(O)	1.38%	Z	3(N)	4.82%	Z	2(O)	1.71%
Z	3(N)	3.33%	Z	3(N)	0.92%	Z	3(N)	2.47%	Z	3(N)	1.13%
Z	5(O)	0.92%	Z	3(N)	1.54%	Z	5(O)	1.95%	Z	3(N)	1.88%
Z	5(O)	1.68%	Z	5(O)	2.16%	Z	5(O)	3.60%	Z	3(N)	0.57%
Z	5(O)	1.11%	Z	5(O)	3.57%	Z	5(O)	2.43%	Z	5(O)	1.81%
			Z	5(O)	2.00%				Z	5(O)	3.00%
									Z	5(O)	1.76%
α_n = 0% β_π = 100%			α_n = 0% β_π = 100%			α_n = 0% β_π = 100%			α_n = 0% β_π = 100%		

Table S16 Calculated configuration proportions of α_n and β_π of **A2**'s various states based on MPA

S_1^{MIN}						T_1^{MIN}					
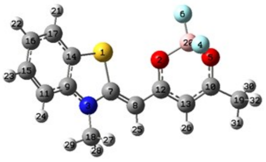						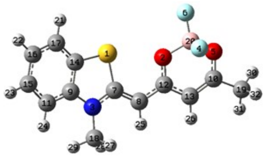					
HOMO			LOMO			HOMO			LOMO		
Type	Atom	Total	Type	Atom	Total	Type	Atom	Total	Type	Atom	Total
Z	1(S)	2.56%	Z	1(S)	1.16%	Z	1(S)	2.27%	Z	1(S)	1.24%
Y	1(S)	0.53%	Z	1(S)	3.02%	Z	1(S)	6.44%	Z	1(S)	3.29%
Z	1(S)	7.25%	Z	1(S)	0.84%	Z	1(S)	1.36%	Z	1(S)	0.98%
Z	1(S)	1.60%	Z	2(O)	1.85%	Z	3(N)	1.97%	Z	2(O)	1.74%
Z	3(N)	2.21%	Z	2(O)	3.07%	Z	3(N)	3.66%	Z	2(O)	2.88%
Z	3(N)	4.11%	Z	2(O)	1.53%	Z	3(N)	2.03%	Z	2(O)	1.46%
Z	3(N)	2.3%	Z	3(N)	1.11%	Z	5(O)	1.76%	Z	3(N)	1.26%
Z	5(O)	1.20%	Z	3(N)	1.82%	Z	5(O)	3.24%	Z	3(N)	2.06%
Z	5(O)	2.19%	Z	3(N)	0.67%	Z	5(O)	2.15%	Z	3(N)	0.89%
Z	5(O)	1.43%	Z	5(O)	1.86%				Z	5(O)	1.54%
			Z	5(O)	3.09%				Z	5(O)	2.55%
			Z	5(O)	1.69%				Z	5(O)	1.40%
α_n = 0.53% β_π = 99.47%			α_n = 0% β_π = 100%			α_n = 0% β_π = 100%			α_n = 0% β_π = 100%		

Table S17 Calculated configuration proportions of α_n and β_π of **A3**'s various states based on MPA

<table>
<tr><td colspan="6">S_1^{MIN}</td><td colspan="6">T_1^{MIN}</td></tr>
<tr><td colspan="6">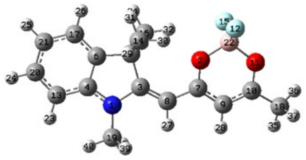</td><td colspan="6">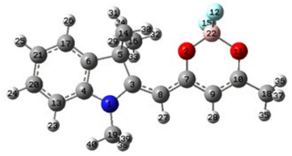</td></tr>
<tr><td colspan="3">HOMO</td><td colspan="3">LOMO</td><td colspan="3">HOMO</td><td colspan="3">LOMO</td></tr>
<tr><td>Type</td><td>Atom</td><td>Total</td><td>Type</td><td>Atom</td><td>Total</td><td>Type</td><td>Atom</td><td>Total</td><td>Type</td><td>Atom</td><td>Total</td></tr>
<tr><td>Z</td><td>1(N)</td><td>4.85%</td><td>Z</td><td>1(N)</td><td>1.09%</td><td>Z</td><td>1(N)</td><td>4.36%</td><td>Z</td><td>1(N)</td><td>1.50%</td></tr>
<tr><td>Z</td><td>1(N)</td><td>9.12%</td><td>Z</td><td>1(N)</td><td>1.87%</td><td>Z</td><td>1(N)</td><td>8.18%</td><td>Z</td><td>1(N)</td><td>2.56%</td></tr>
<tr><td>Z</td><td>1(N)</td><td>5.40%</td><td>Z</td><td>1(N)</td><td>0.58%</td><td>Z</td><td>1(N)</td><td>4.58%</td><td>Z</td><td>1(N)</td><td>0.92%</td></tr>
<tr><td>Z</td><td>11(O)</td><td>0.85%</td><td>Z</td><td>2(O)</td><td>2.05%</td><td>Z</td><td>11(O)</td><td>1.20%</td><td>Z</td><td>2(O)</td><td>1.66%</td></tr>
<tr><td>Z</td><td>11(O)</td><td>0.55%</td><td>Z</td><td>2(O)</td><td>3.42%</td><td>Z</td><td>11(O)</td><td>2.19%</td><td>Z</td><td>2(O)</td><td>2.77%</td></tr>
<tr><td></td><td></td><td></td><td>Z</td><td>2(O)</td><td>1.88%</td><td>Z</td><td>11(O)</td><td>1.45%</td><td>Z</td><td>2(O)</td><td>1.53%</td></tr>
<tr><td></td><td></td><td></td><td>Z</td><td>11(O)</td><td>2.11%</td><td></td><td></td><td></td><td>Z</td><td>11(O)</td><td>1.81%</td></tr>
<tr><td></td><td></td><td></td><td>Z</td><td>11(O)</td><td>3.50%</td><td></td><td></td><td></td><td>Z</td><td>11(O)</td><td>3.01%</td></tr>
<tr><td></td><td></td><td></td><td>Z</td><td>11(O)</td><td>1.92%</td><td></td><td></td><td></td><td>Z</td><td>11(O)</td><td>1.70%</td></tr>
<tr><td colspan="3">$\alpha_n = 0\%$
$\beta_\pi = 100\%$</td><td colspan="3">$\alpha_n = 0\%$
$\beta_\pi = 100\%$</td><td colspan="3">$\alpha_n = 0\%$
$\beta_\pi = 100\%$</td><td colspan="3">$\alpha_n = 0\%$
$\beta_\pi = 100\%$</td></tr>
</table>

Table S18 Calculated configuration proportions of α_n and β_π of **A4**'s various states based on MPA

<table>
<tr><td colspan="6">S_1^{MIN}</td><td colspan="6">T_1^{MIN}</td></tr>
<tr><td colspan="6">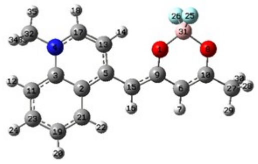</td><td colspan="6">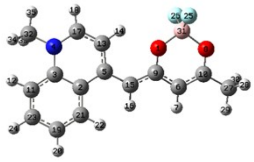</td></tr>
<tr><td colspan="3">HOMO</td><td colspan="3">LOMO</td><td colspan="3">HOMO</td><td colspan="3">LOMO</td></tr>
<tr><td>Type</td><td>Atom</td><td>Total</td><td>Type</td><td>Atom</td><td>Total</td><td>Type</td><td>Atom</td><td>Total</td><td>Type</td><td>Atom</td><td>Total</td></tr>
<tr><td>Z</td><td>4(N)</td><td>2.01%</td><td>Z</td><td>1(O)</td><td>0.68%</td><td>Z</td><td>4(N)</td><td>2.17%</td><td>Z</td><td>1(O)</td><td>0.72%</td></tr>
<tr><td>Z</td><td>4(N)</td><td>3.64%</td><td>Z</td><td>1(O)</td><td>1.16%</td><td>Z</td><td>4(N)</td><td>3.95%</td><td>Z</td><td>1(O)</td><td>1.22%</td></tr>
<tr><td>Z</td><td>4(N)</td><td>1.89%</td><td>Z</td><td>1(O)</td><td>0.70%</td><td>Z</td><td>4(N)</td><td>2.09%</td><td>Z</td><td>1(O)</td><td>0.73%</td></tr>
<tr><td>Z</td><td>8(O)</td><td>2.02%</td><td>Z</td><td>4(N)</td><td>1.83%</td><td>Z</td><td>8(O)</td><td>1.84%</td><td>Z</td><td>4(N)</td><td>1.80%</td></tr>
<tr><td>Z</td><td>8(O)</td><td>3.70%</td><td>Z</td><td>4(N)</td><td>3.03%</td><td>Z</td><td>8(O)</td><td>3.37%</td><td>Z</td><td>4(N)</td><td>2.97%</td></tr>
<tr><td>Z</td><td>8(O)</td><td>2.49%</td><td>Z</td><td>4(N)</td><td>1.25%</td><td>Z</td><td>8(O)</td><td>2.26%</td><td>Z</td><td>4(N)</td><td>1.22%</td></tr>
<tr><td></td><td></td><td></td><td>Z</td><td>8(O)</td><td>0.68%</td><td></td><td></td><td></td><td>Z</td><td>8(O)</td><td>0.80%</td></tr>
<tr><td></td><td></td><td></td><td>Z</td><td>8(O)</td><td>1.16%</td><td></td><td></td><td></td><td>Z</td><td>8(O)</td><td>1.36%</td></tr>
<tr><td></td><td></td><td></td><td>Z</td><td>8(O)</td><td>0.72%</td><td></td><td></td><td></td><td>Z</td><td>8(O)</td><td>0.84%</td></tr>
<tr><td colspan="3">$\alpha_n = 0\%$
$\beta_\pi = 100\%$</td><td colspan="3">$\alpha_n = 0\%$
$\beta_\pi = 100\%$</td><td colspan="3">$\alpha_n = 0\%$
$\beta_\pi = 100\%$</td><td colspan="3">$\alpha_n = 0\%$
$\beta_\pi = 100\%$</td></tr>
</table>

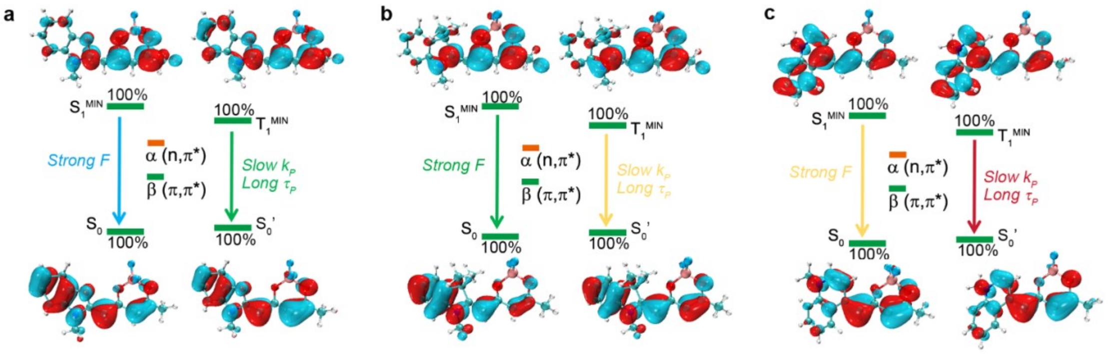

Fig. S21 Proportions of (π,π*) configuration and molecular orbital profiles of **A1** (a), **A3** (b), and **A4** (c) at different states.

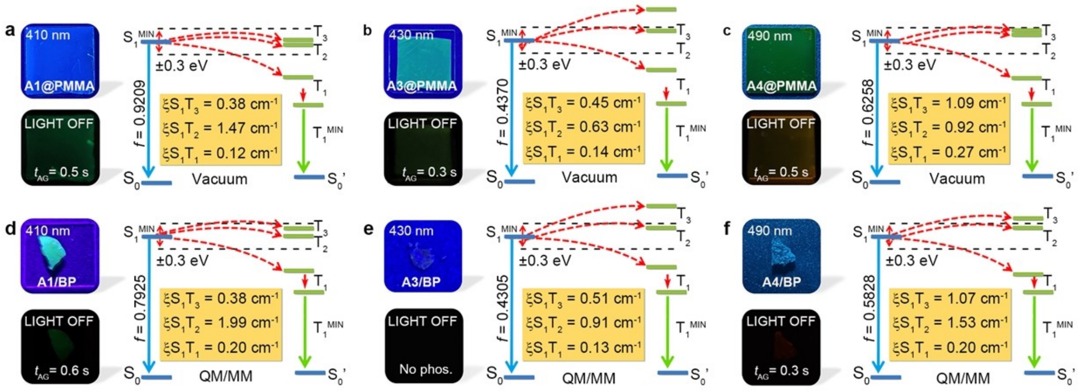

Fig. S22 Calculated SOCs of **A1** (a), **A3** (b), and **A4** (c) under vacuum conditions and fluorescence and afterglow photographs of **A1@PMMA**, **A3@PMMA**, and **A4@PMMA** (1 wt%) under vacuum. Calculated SOCs of **A1** (d), **A3** (e), and **A4** (f) and fluorescence and afterglow photographs of **A1/BP**, **A3/BP**, and **A4/BP**. (Ex = 410 nm (**A1**), 430 nm (**A3**), and 490 (**A4**) nm)

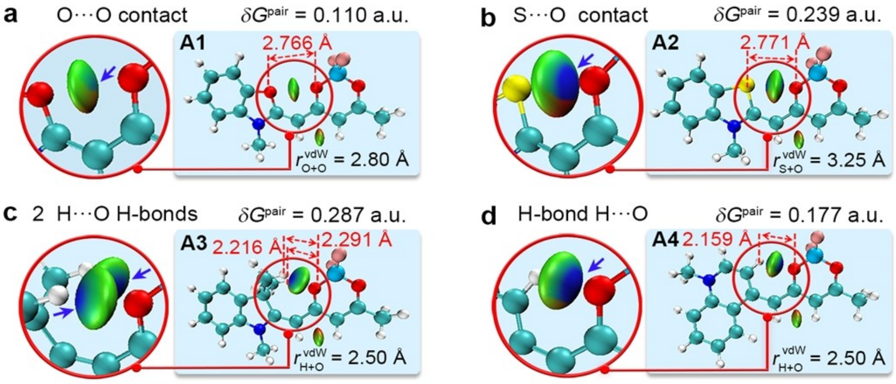

Fig. S23 (a) IGMH maps of the two fragments in **A1**–**A4** in single crystals with *Sign*(λ_2)ρ-coloured isosurfaces of δg^{inter} = 0.006 a.u. (Interatomic distance, sum of van der Waals radii, and δG^{pair} indices are labelled.)

7. NMR and HRMS spectra of **A1**–**A4**

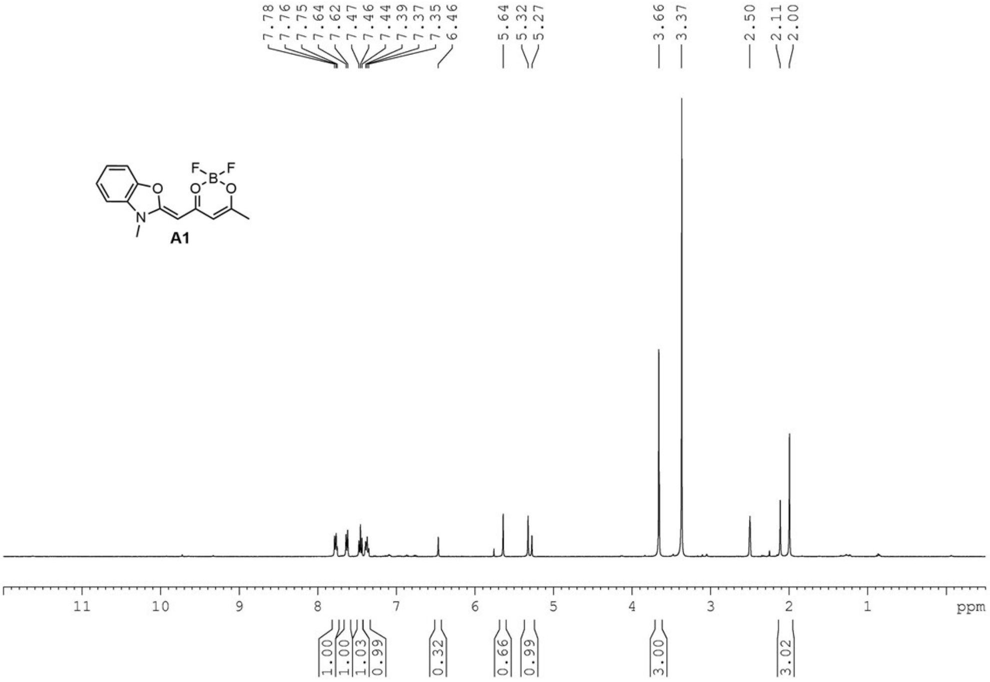

Fig. S24 ^{1}H NMR spectrum of **A1**.

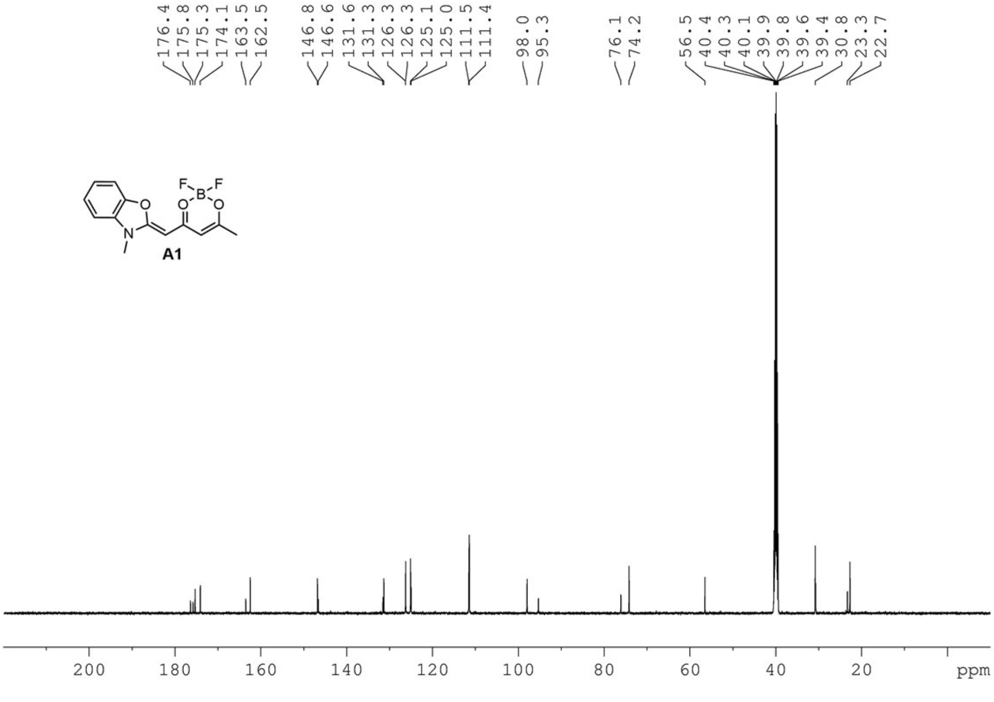

Fig. S25 ^{13}C NMR spectrum of **A1**.

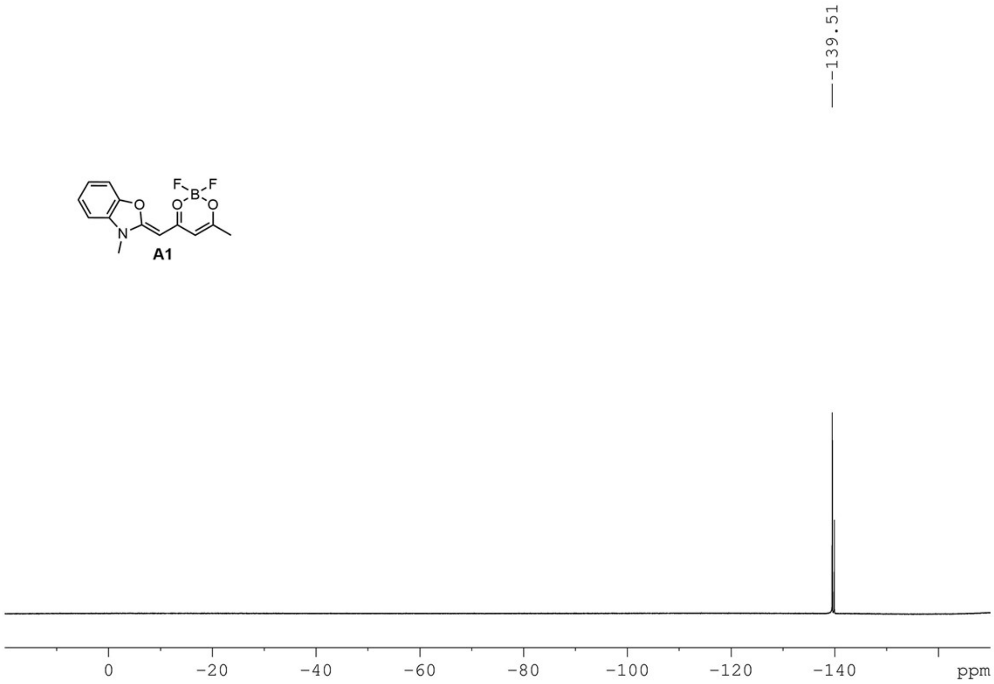

Fig. S26 ^{19}F NMR spectrum of **A1**.

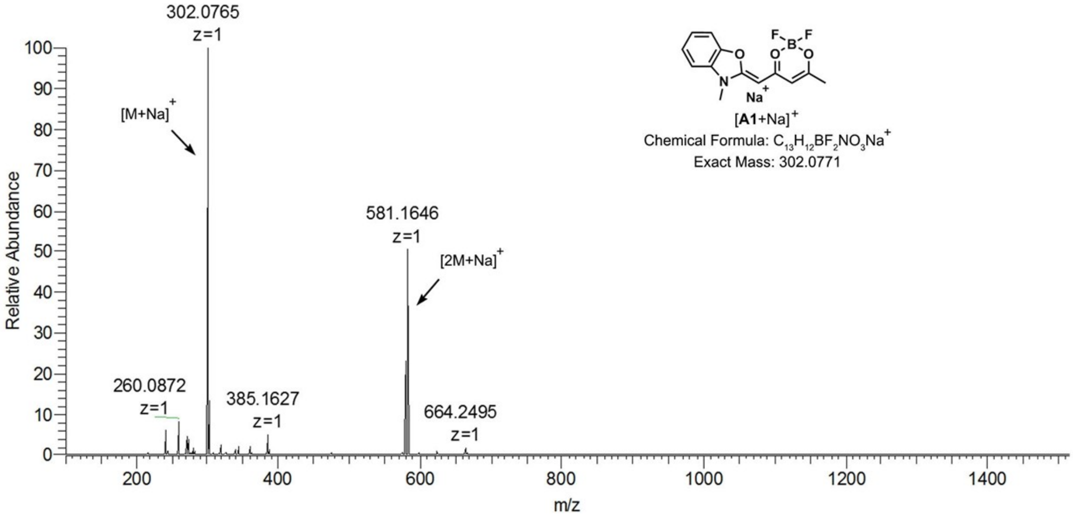

Fig. S27 HRMS spectrum of **A1**.

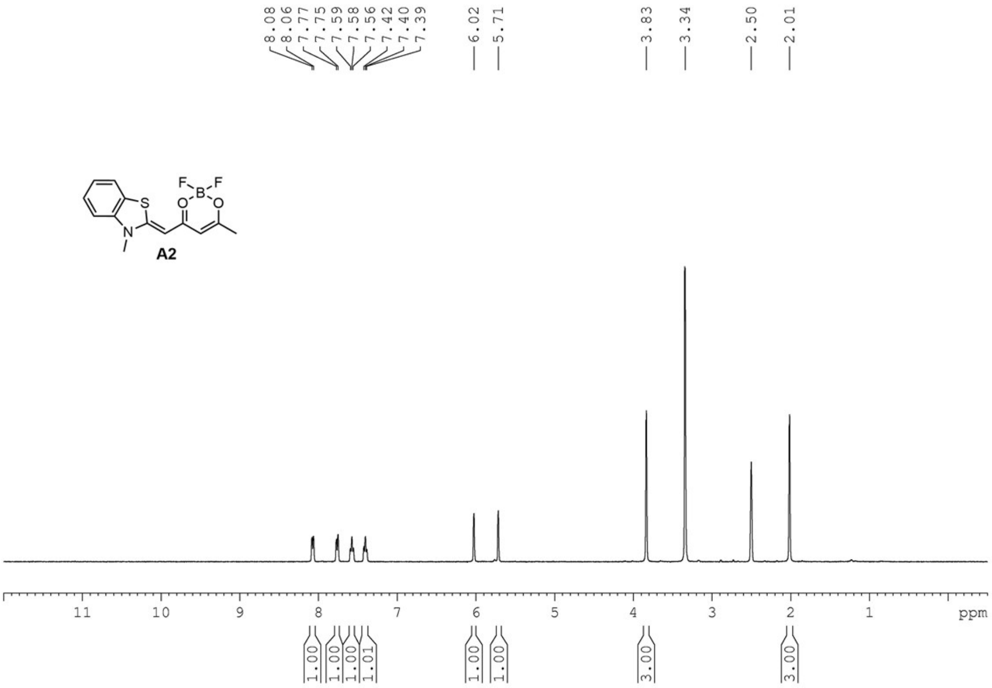

Fig. S28 ^{1}H NMR spectrum of **A2**.

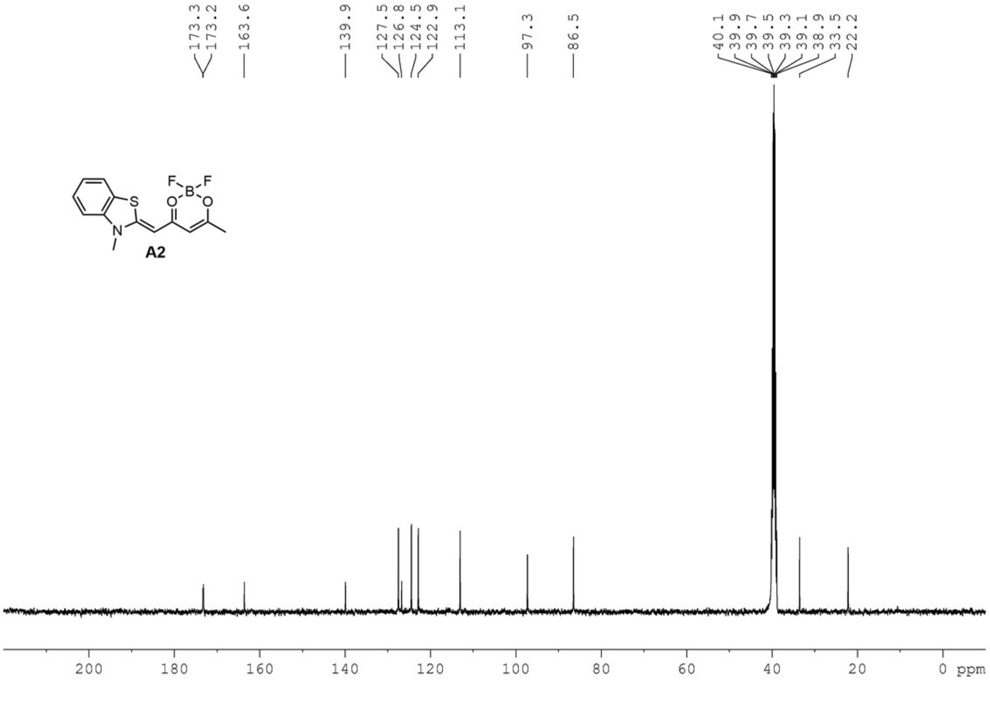

Fig. S29 ^{13}C NMR spectrum of **A2**.

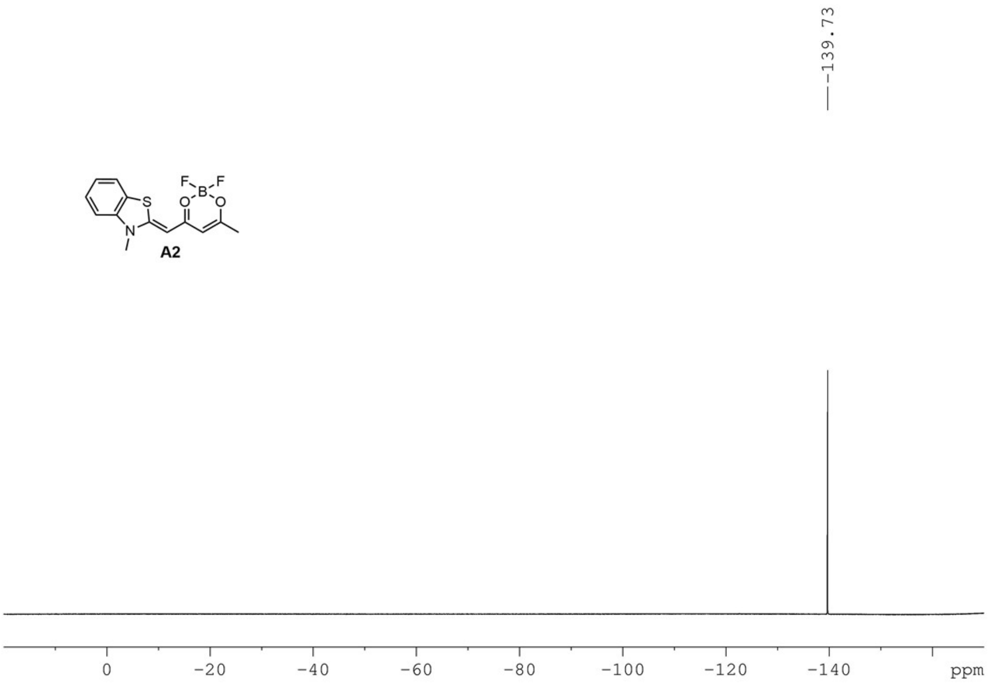

Fig. S30 ^{19}F NMR spectrum of **A2**.

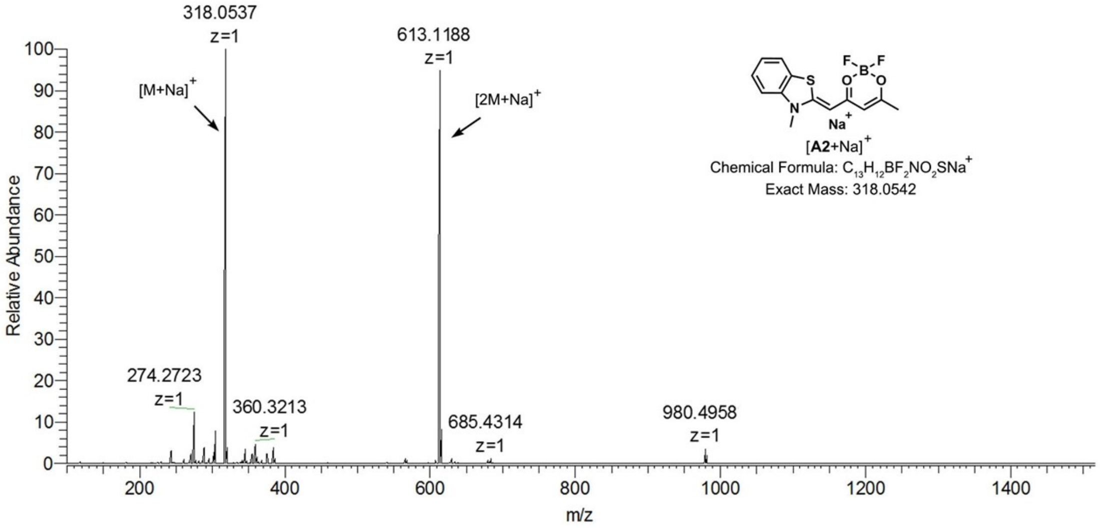

Fig. S31 HRMS spectrum of **A2**.

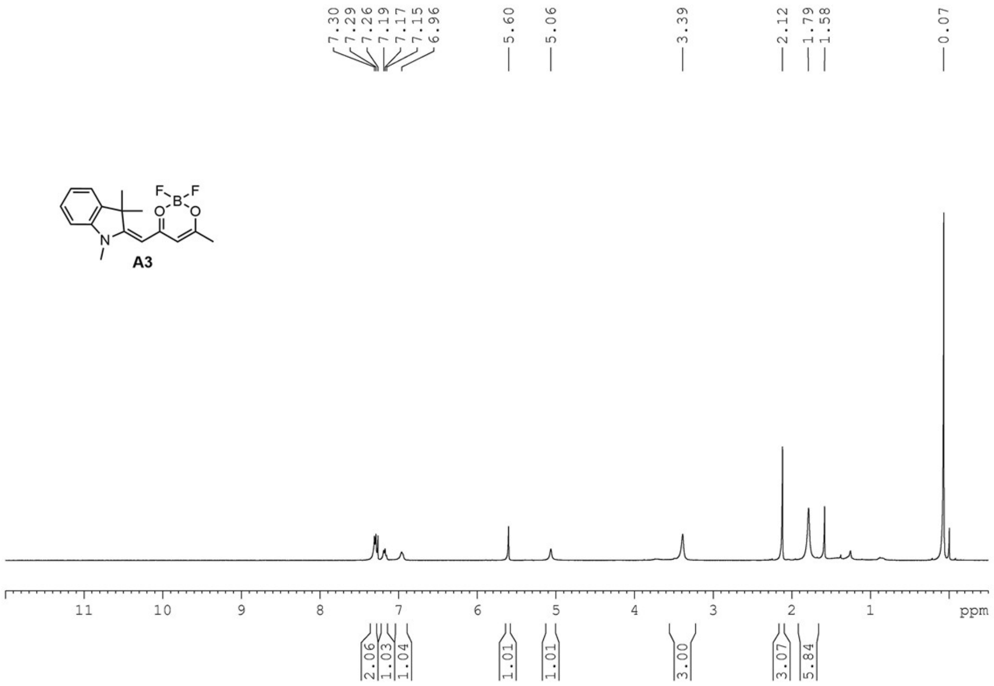

Fig. S32 ^{1}H NMR spectrum of **A3**.

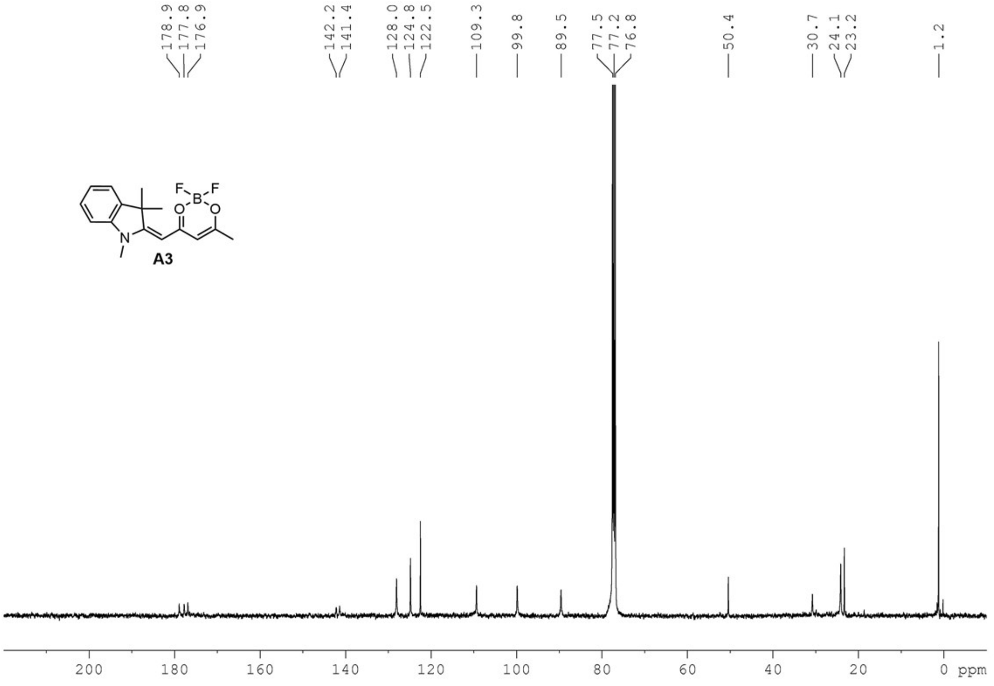

Fig. S33 ^{13}C NMR spectrum of **A3**.

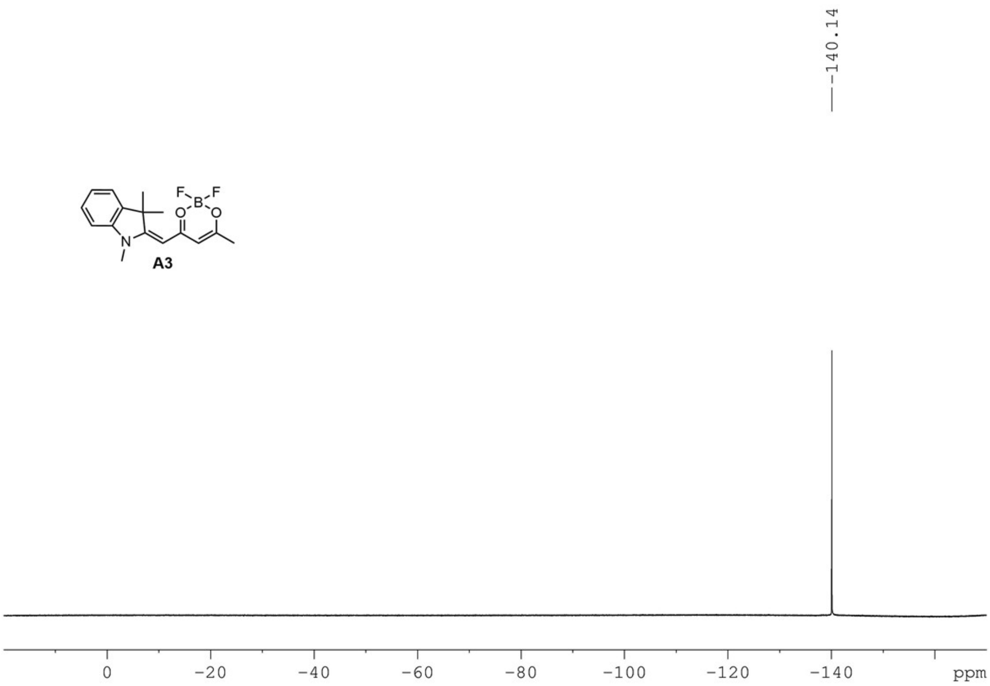

Fig. S34 ^{19}F NMR spectrum of **A3**.

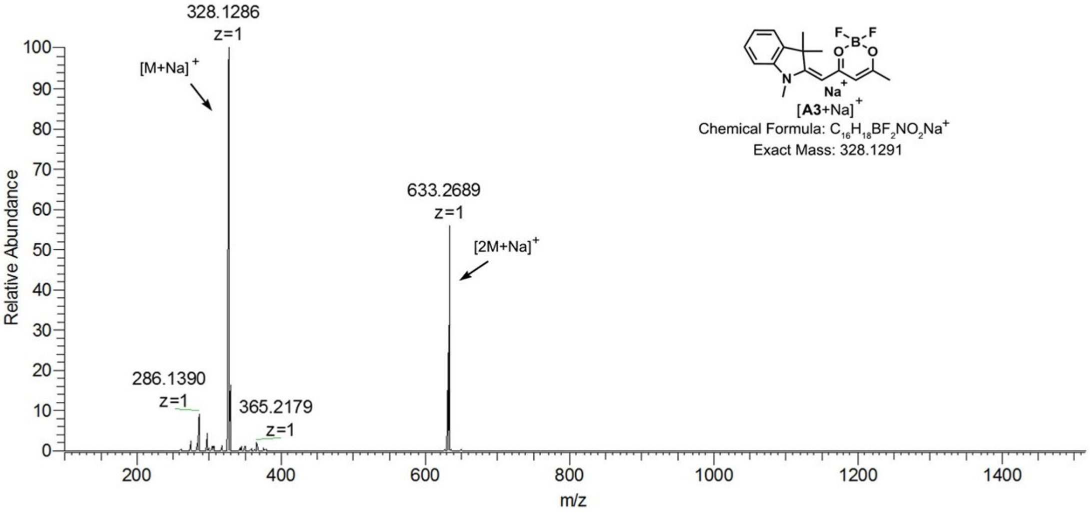

Fig. S35 HRMS spectrum of **A3**.

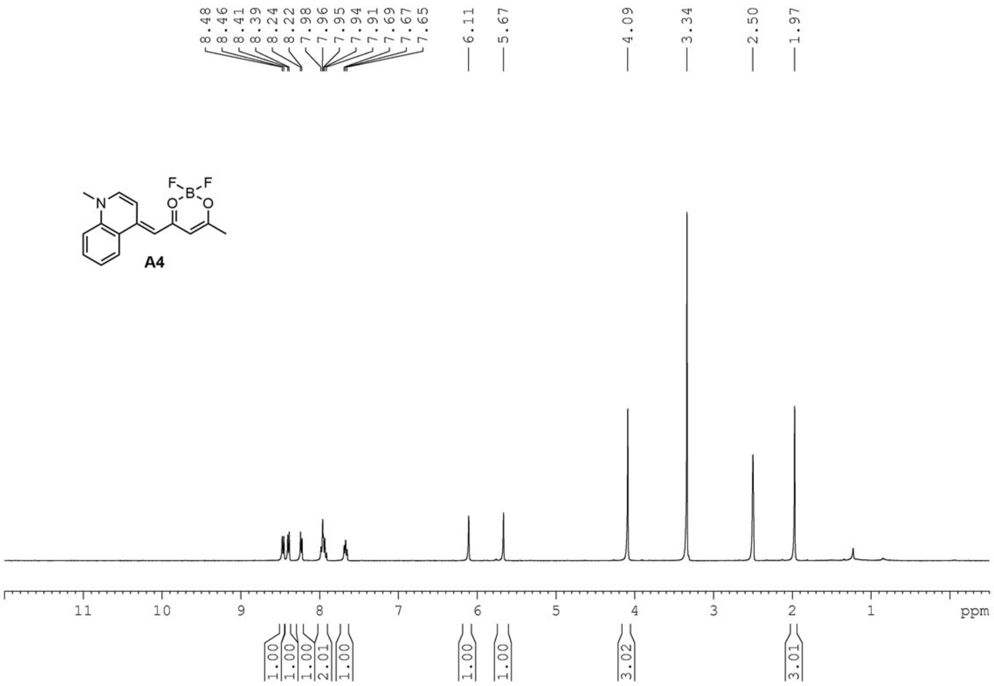

Fig. S36 ^{1}H NMR spectrum of **A4**.

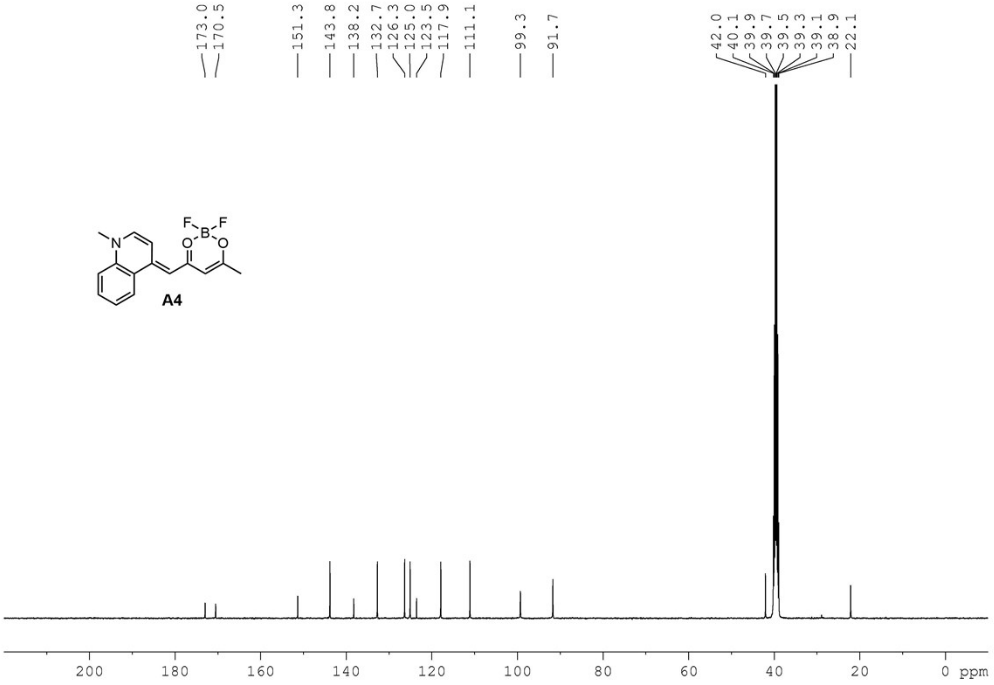

Fig. S37 ^{13}C NMR spectrum of **A4**.

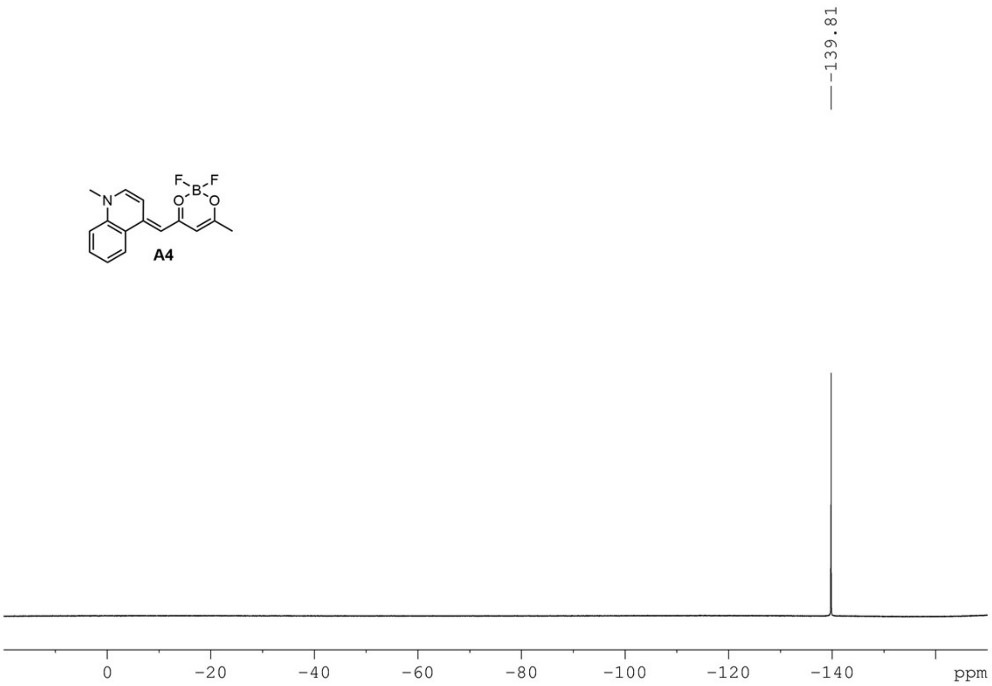

Fig. S38 ^{19}F NMR spectrum of **A4**.

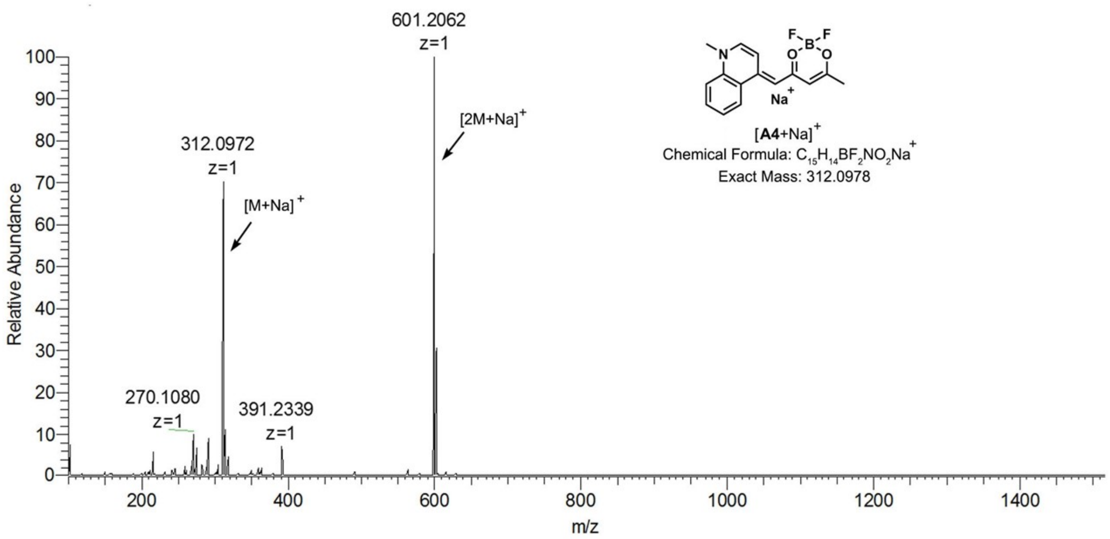

Fig. S39 HRMS spectrum of **A4**.

8. HPLC purity analysis of **A1**–**A4**

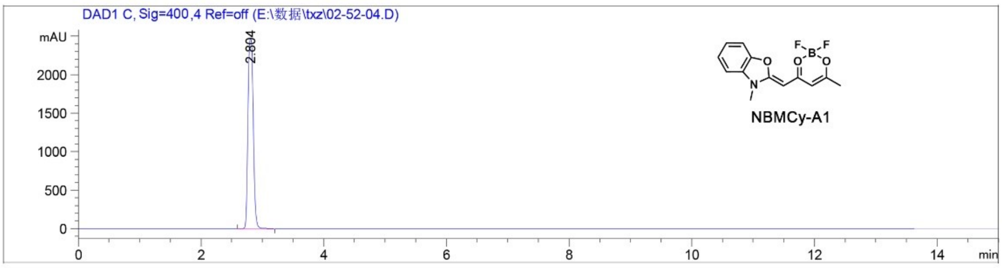

Fig. S40 HPLC trace of **A1**.

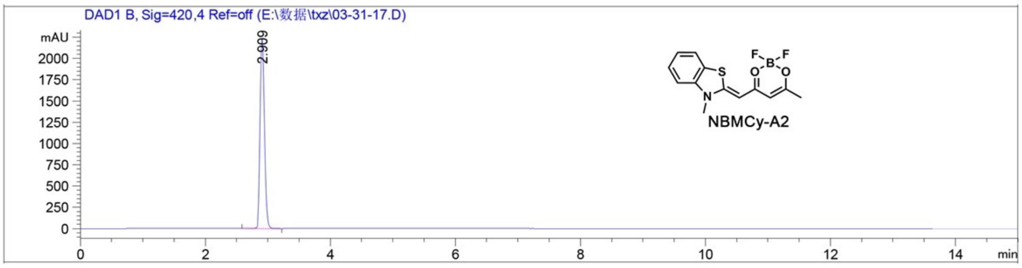

Fig. S41 HPLC trace of **A2**.

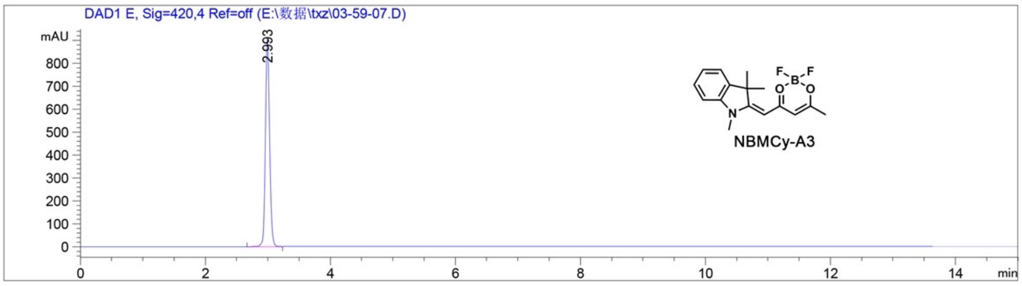

Fig. S42 HPLC trace of **A3**.

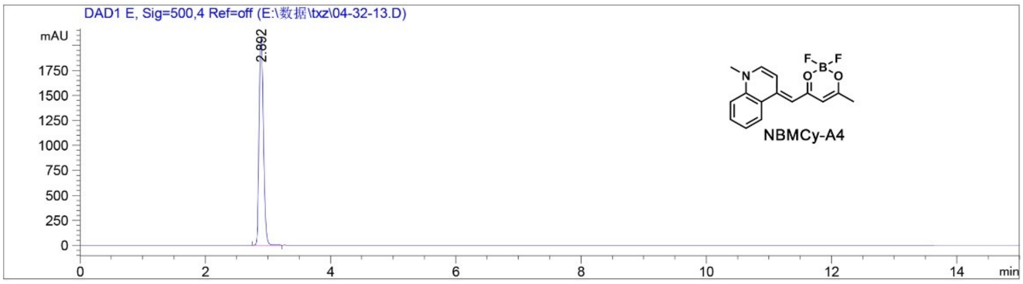

Fig. S43 HPLC trace of **A4**.